REAL-TIME PCR METHOD FOR THE DETECTION OF CYTOKINE EXPRESSION IN HUMAN PROINFLAMMATORY T CELLS

Master's Thesis
Iina Vainio
Institute of Medical Technology
University of Tampere
2009

ACKNOWLEDGEMENTS

This study was done in the Virology Research Group in the University of Tampere. I would like to thank Professor Heikki Hyöty for conducting my Master's thesis in his study group and for his advice during the project. I would also like to thank M.Sc. Hanna Honkanen for supervising this study and for all the useful advice she gave. I also express my gratitude to the technicians of the Virology Research Group for the assistance in the laboratory work. The whole personnel of the Virology Research Group deserve many thanks for their support and help.

I would also like to thank my close relatives and friends for their support and encouragement during this study.

PRO GRADU- TUTKIELMA

Paikka:	TAMPEREEN YLIOPISTO Lääketieteellinen tiedekunta Lääketieteellisen teknologian instituutti
Tekijä:	VAINIO, IINA LEENA MAARIA
Otsikko:	Real-time PCR method for the detection of cytokine expression in human proinflammatory T cells
Sivumäärä:	61 sivua
Ohjaajat:	Professori Heikki Hyöty (LT) ja laboraattori Hanna Honkanen (FM)
Tarkastajat:	Professorit Markku Kulomaa ja Heikki Hyöty (LT)
Aika:	Marraskuu 2009

TIIVISTELMÄ

Tutkimuksen tausta ja tavoitteet: Immuunijärjestelmän toimintahäiriöihin liittyvät sairaudet, kuten allergiat ja autoimmuunisairaudet, ovat yleistyneet viime vuosikymmenien aikana kehittyneissä maissa. Suomessa on maailman suurin tyypin 1 diabeteksen esiintyvyys, jonka arvellaan johtuvan osittain geneettisistä ja osittain ympäristötekijöistä, kuten HLA-geeneistä ja enterovirusinfektiosta. Immunologisissa sairauksissa esiintyy monenlaisia immuunijärjestelmän toimintahäiriöitä, jotka ilmenevät lymfosyyttien erittämien sytokiinien pitoisuuksien muutoksina ja proinflammatoristen T-solujen voimistuneina vasteita. Tämän tutkimuksen tavoitteena oli optimoida reaaliaikainen PCR-menetelmä kolmen proinflammatorisen sytokiinin määrittämiseen, ja löytää toimiva RNA:n eristysmenetelmä erityyppisille valkosolunäytteille. Lopullisena tavoitteena oli kehittää menetelmä, jolla voidaan luotettavasti määrittää sytokiinien ilmenemistä immunologisissa sairauksissa ja infektiotaudeissa.

Tutkimusmenetelmät: Verinäytteet saatiin joko terveiltä vapaaehtoisilta tai DIPP-tutkimukseen osallistuvilta lapsilta. Veren sisältämät valkosolut puhdistettiin kahdella eri tavalla: mononukleaarisina leukosyytteinä tai nk. buffy-coat–soluina. Näytteistä eristettiin RNA, joka käännettiin cDNA:ksi RT-reaktiolla. Näin saatu cDNA, joka sisälsi tutkittavia sytokiineja koodaavan mRNA:n, monistettiin tässä tutkimuksessa kehitetyillä reaaliaikaisilla PCR-menetelmillä. Näin voitiin määrittää sytokiinien ilmentymistä joko absoluuttisesti tai suhteellisesti hyödyntämällä Pfafflin matemaattista mallia. Tulokset varmistettiin agaroosigeelielektroforeesilla.

Tutkimustulokset: Reaaliaikainen PCR-menetelmä optimoitiin onnistuneesti kolmelle tärkeälle proinflammatoriselle sytokiinille (interferoni-gamma, interleukiini-4 ja interleukiini-17). RNA:n eristys jäädytetyistä buffy-coat näytteistä saatiin toimimaan parhaiten Qiagen RNeasy® Mini Kitin muokatuilla protokollilla. Lisäksi *in vitro* valkosolustimulaatioissa määritettiin stimuloitujen T-solujen sytokiinien ilmentymistä, jolloin havaittiin tiettyjen enterovirusten aktivoivan autoimmuunisairauksiin liitettyjä proinflammatorisia vasteita.

Johtopäätökset: Tässä tutkimuksessa kehitettiin reaaliaikainen PCR–menetelmä, jota voidaan luotettavasti käyttää sytokiinien ilmenemisen määrittämiseen ihmisen valkosoluista laajoissa seurantatutkimuksissa, kuten DIPP-tutkimuksessa, ja *in vitro* tehtävissä valkosolustimulaatioissa. Menetelmä mahdollistaa sytokiinivasteen tutkimisen sekä immunologisissa sairauksissa että soluviljelmissä aktivoidussa valkosoluissa.

MASTER'S THESIS

Place:	UNIVERSITY OF TAMPERE Faculty of Medicine Institute of Medical Technology (IMT)
Author:	VAINIO, IINA LEENA MAARIA
Title:	Real-time PCR method for the detection of cytokine expression in human proinflammatory T cells
Pages:	61 pp.
Supervisors:	Professor Heikki Hyöty (MD) and Laboratory Manager Hanna Honkanen (MSc)
Reviewers:	Professors Markku Kulomaa and Heikki Hyöty (MD)
Date:	November 2009

ABSTRACT

Background and Aims: Immune-mediated diseases such as allergies and autoimmune diseases have increased during the past decades in developed countries. The incidence of type 1 diabetes is very high in Finland and both genetic and environmental factors, such as HLA genes and enteroviruses, are probably contributing to this phenomenon. Immunopathology of immune-mediated diseases is mediated by proinflammatory T cells, which can secrete several cytokines to contribute the tissue damage. Accordingly, imbalances in differentiation and function of the T cells are commonly observed in patients. The aim of this study was to create a panel of real-time PCR methods, which can detect cytokine expression of human proinflammatory T cells. Another aim was to optimize RNA extraction methods for stored buffy-coat samples, which have been collected in large clinical studies. The final goal of this study was to develop methods which can be used for the analyses of cytokine expression in different clinical conditions like acute virus infections and immune-mediated diseases.

Methods: Human blood samples were obtained from healthy volunteers or from the children participating in the prospective DIPP study. White blood cells were purified from blood samples either as mononuclear cells or as buffy-coat. RNA was isolated from fresh and stored white blood cells using different commercial assays and RNA was transcripted into cDNA with RT-reaction. cDNA was then used as a template in real-time PCR to measure interferon-gamma, interleukin-4 and interleukin-17 mRNA expression. The relative gene expression was calculated with Pfaffl equation and the results were confirmed by agarose gel electrophoresis.

Results: The real-time PCR was optimized successfully for three proinflammatory cytokines. RNA isolation from frozen buffy-coat samples worked best with modified protocols of Qiagen RNeasy® Mini Kit. Optimized assays were then used to analyze the effect of enteroviruses on cytokine expression. The *in vitro* white blood cell stimulations revealed that some enterovirus serotypes induced clear increases in the cytokines which are associated with autoimmune diseases.

Conclusions: New real-time PCR assays were developed for the detection of three important proinflammatory cytokines. These real-time PCR methods can be reliably used for the detection of both basal and stimulated expression of proinflammatory cytokines in human white blood cells.

TABLE OF CONTENTS

ABBREVIATIONS

bp	Base pair
cDNA	Complementary DNA
CT	Cycle threshold
DIPP study	Diabetes Prediction and Prevention study
HLA	Human leukocyte antigen
IgE	Immunoglobulin E
IFN-γ	Interferon-gamma
IL-4	Interleukin-4
IL-17	Interleukin-17
TRC	T cell receptor
Real-time PCR	Real-time polymerase chain reaction
RT reaction	Reverse transcription reaction / Reverse transcription –polymerase chain reaction
TBP	TATA binding protein
T_H cells	T helper cells (T_H1, T_H2 and T_H17 cells)
T_{reg} cells	Regulatory T cells (T_R1 and nT_{reg} cells)
nT_{reg} cells	Natural T regulatory cells
T_m	Melting temperature of the primers

1. INTRODUCTION

During the recent decades the failures in immune regulation, such as autoimmune diseases and allergies, have become more common in developed countries because of genetic and environmental factors (Bach, 2002). For example, the incidence of childhood type 1 diabetes mellitus is the highest in Finland, a phenomenon which may be linked to both specific HLA (Human leukocyte antigen) risk genes and environmental factors. For example, lack of microbial infections, as suggested by hygiene hypothesis, can modulate the risk of the disease. (Kondrashova et al., 2005) Moreover, enterovirus infections seem to correlate with increased risk of type 1 diabetes (Richman et al., 2002). Due to a high incidence of type 1 diabetes, Finland is an optimal area to study immunological diseases. Finnish DIPP (Diabetes Prediction and Prevention) study screens newborns for HLA risk alleles for type 1 diabetes and aims to predict and search for means to delay and prevent type 1 diabetes in a large population-based cohort. (Kupila et al., 2001) Knowing the molecular mechanisms underlying the failures in immune regulation gives valuable information about the pathogenesis of these diseases and their possible new treatment strategies.

Immune-mediated diseases are associated with an abnormal function of immune system. Many immune-mediated diseases are characterized by increased proinflammatory responses mediated by proinflammatory T_H cells (T helper cells). On the other hand the regulatory arm of the immune system is also important and abnormal function of T_{reg} cells (regulatory T cells) can lead to immunological diseases. Thus, the balance of activation, regulation, differentiation and function of different T_H cell lineages are connected to immunological disorders. (Dong, 2008) This study concentrates on the proinflammatory immune system and the hallmark cytokines that the different T_H cell lineages (T_H1, T_H2 and T_H17 cells) express to mediate their function.

The relative gene expression of the proinflammatory cytokines can be analyzed using real-time PCR (real-time polymerase chain reaction), which enables simultaneous amplification and detection of specific DNA sequences by fluorescence technique (Kubista et al., 2006). The real-time PCR is harnessed in this study to detect three important proinflammatory cytokines, each representing one of the T_H cell lineages, from human white blood cell samples.

First, the background related to differentiation of T cells, regulation of immune system and conditions related to abnormal function of immune system are presented. In addition, the real-time PCR procedure and RNA isolation methods are introduced. The results of this study are focused on the optimization of the real-time PCR, RNA isolation from buffy-coat samples and *in vitro* stimulations of white blood cells. Finally, the interpretations of the results are described.

2. REWIEV OF THE LITERATURE

2.1. T cells and immune system

The main function of the immune system and white blood cells, such as T cells, is to protect the body from invading pathogens and microorganisms by destroying the pathogens and infected cells while minimizing the damage to tissues (Cools et al., 2007). There are five major immunological T cell lineages (Figure 1) that are defined according to following criteria. First, the naïve cells differentiate independently into each lineage *in vivo* and *in vitro* and second, each lineage has gene expression signature that is distinct and heritable. So, $CD4^+$ T cells differentiate into different T cell lineages that have distinct gene expression, regulation and biological function. T_H cells and T_{reg} cells are important in our understanding of the molecular mechanisms involved in development of immune regulation failures. (Dong, 2008)

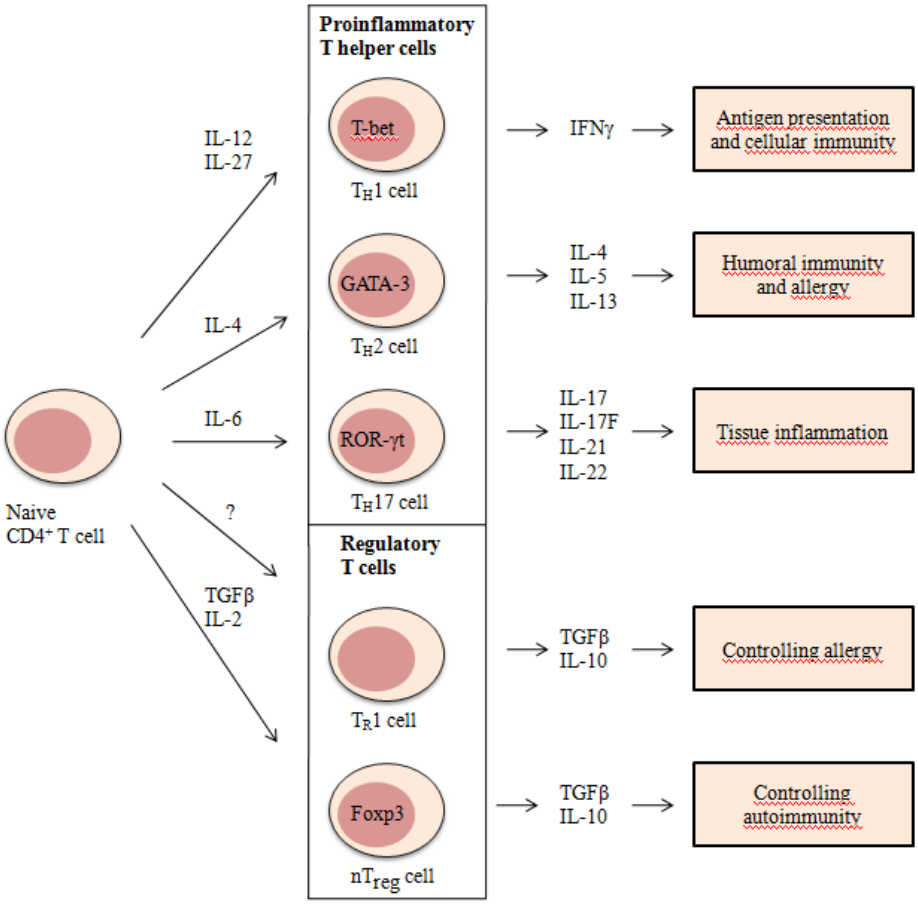

Figure 1. Scheme of T cell differentiation in humans. Modified from Dong, 2008 and Oboki et al., 2008.

2.1.1. T cell differentiation in human and mouse

The differentiation of proinflammatory T_H cells (T_H1, T_H2 and T_H17) is driven by signals originating from T cell and co-stimulatory receptors as well as from cytokines of the surroundings produced by already activated T_H cells. This differentiation process is finely balanced. (Rautajoki et al., 2008) There are some differences in T cell differentiation between human and mouse. The differentiation pathways are well known in mice, but still unsolved questions considering human T cell differentiation exist. The human T cell differentiation is represented in Figure 1. During T cell differentiation epigenetic changes in the chromosome occur, for example, across IFN-γ (interferon-gamma) gene in T_H1 cells and across IL-4 (interleukin-4) gene in T_H2 cells (Rautajoki et al., 2008).

Human naïve $CD4^+$ T cells differentiate into T_H1 cells in the presence of IL-12 and IL-27, into T_H2 cells in the presence of IL-4 and into T_H17 cells in the presence of IL-6. The mechanisms in human T_R1 cell differentiation remain unclear, but nT_{reg} cells (natural regulatory T cells) are differentiated through TGFβ and IL-2 mediated pathways (Figure 1). (Oboki et al., 2008)

The comparable T cell differentiation in mice model is considered as following. In mouse IL-12 or IL-27 induce the naïve $CD4^+$ T cell differentiation into T_H1 cells and IL-4, TSLP or IL-25 into T_H2 cells. T_H17 cells are formed in the presence of IL-23 after action of TGF-β1 and IL-6 or after IL-21-mediated cell differentiation. Naïve T cells differentiate into T_R1 cells in the presence of IL-27 after action of TGF-β1 and IL-6 or after IL-21-mediated cell differentiation. nT_{reg} cells differentiation is induced by TGF-β1 and IL-2. (Oboki et al., 2008) IL-23 was originally shown to be important for the proliferation of T_H17 cells and for T_H17 cell-mediated immune diseases. However, it does not seem to be necessary for the initiation of T_H17 cell differentiation. (Dong, 2008)

The molecular mechanisms of human T_H cell differentiation include the following complex cascades. IL-12 is produced mainly by macrophages and dendritic cells, but also by monocytes, neutrophils and B cells as a response to invasive pathogens. Naïve T_H cells lack IL-12 receptor β2 (IL-12β2) expression, which forms IL-12 receptor together with IL-12β1. Human TCR (T cell receptor) signaling and STAT4 induce IL-12β2 expression. IL-27 is a novel cytokine also related to T_H1 cell differentiation trough phosphorylation of STAT1 both in human and mouse. In addition, IFN-γ produced in response to bacteria and viruses promotes T_H1 cell differentiation also via STAT1 signaling pathway. T-bet alias TBX21 is a transcription factor, that binds to DNA through

its T-box DNA binding domain, repressing production of T_H2 cytokines and mediating production of the T_H1 hallmark cytokine IFN-γ. IL-4, produced by many cell types such as mast cells, basophils, eosinophils, natural killer cells and differentiated T_H2 cells, signals through IL-4 receptor (IL-4R) promoting T_H2 cell differentiation. $CD4^+$ T_H cells produce IL-4 in a STAT6-independent manner during their initial activation in lymph nodes. STAT6 becomes prhosphorylated and dimerized when IL-4 binds its receptor. As a consequence, STAT6 is localized into the nucleus, where it regulates the transcription of its target genes, for example, upregulating GATA3 expression in developing T_H2 cell. GATA3 can induce the production of IL-4 in developing T_H2 cells and it also downregulates the expression of T_H1 type chemokine receptor CXCR3 and upregulates T_H2 type chemokine receptor CCR4. (Rautajoki et al., 2008) The differentiation of T_H17 cells is independent of the STAT signaling pathway, but the process is related to retinoid-related orphan receptor (ROR)-γτ (Chatila et al., 2008).

The innate immune system affects also the T cell differentiation. The innate immune system provides co-stimulatory molecules, for instance, co-stimulatory receptors CD28 and ICOS to enable optimal T cell activation, proliferation and differentiation. (Dong, 2008) In addition, TCR-regulated factors involved in T_H cell differentiation such as NFAT proteins, Tec kinases and caspases have variable effects on the process (Rautajoki et al., 2008).

2.1.2. Proinflammatory immune response

T_H1, T_H2 and T_H17 cells are the key cell types of the proinflammatory immune system. They are important in the immune response to pathogens as well as in the pathogenesis of human immune-mediated diseases. (Rautajoki et al., 2008) Proinflammatory immune system participates in the defense against infections and executes the aggressive immunological action while the T_{reg} cells regulate proinflammatory immune responses.

Proinflammatory T_H cells have an important role in the development of autoimmune diseases and allergies. There are two well known T_H cell types: T_H1 and T_H2 cells. In addition, there is a novel T_H cell type, T_H17 cells. The balance between these different cell lineages influences the development of immune abnormalities such as allergy and autoimmune diseases. The balance between T_HI and T_H2 is moved toward T_H1 pathway in autoimmune diseases while a shift toward T_H2 is linked to allergic disorders. (Dong, 2008) So, the differentiation of naïve $CD4^+$ T cells into

T_H1 or T_H2 cells determines whether humoral or cell-mediated immunity will predominate (Janeway et al., 2005). The role of T_H17 cells is so far unclear, but they may play a significant role in various immunological diseases and tissue inflammation and promote the immune response against infectious agents (Dong, 2008).

2.1.2.1. The role of proinflammatory cytokines IFN-γ, IL-4 and IL-17

The effector cells of the proinflammatory immune system, T_H1, T_H2 and T_H17, express proinflammatoy cytokines to mediate their function (Figure 1). T_H1 cells produce cytokine called IFN-γ and T_H2 cells produce IL-4. IL-17 (interleukin-17) is produced by T_H17 cells. The cytokines act via binding to their specific receptors. For instance, IL-17 binds to and signals through IL-17 receptor A (IL-17RA) that is a member of IL-17R family. IL-17RA is widely expressed by mesenchymal cells such as endothelial cells, epithelial cells and fibroblasts. IL-17RA can also form heterodimers with IL-17RC, that raises possibility of additional receptor forms with different affinity for IL-17 and different signal transduction pathways. (Dong, 2008)

2.1.2.2. T_H1 cells promote antigen presentation and cellular immunity

T_H1 cells act trough cell-mediated immunity. They activate macrophages and induce B cells to produce opsonizing antibody classes such as IgG, which are involved in phagocytosis (Janeway et al., 2005). T_H1 cells are important for the eradication of intracellular pathogens like bacteria, parasites, yeasts and viruses (Rautajoki et al., 2008). High activity of T_H1 cells and increased concentrations of IFN-γ are incriminated in the pathogenesis of autoimmune diseases such as rheumatoid arthritis, multiple sclerosis and type 1 diabetes mellitus (Rabin & Levison, 2008).

2.1.2.3. T_H2 cells and humoral immunity

T_H2 cells mediate protection against extracellular pathogens. They provide humoral immunity where IgM, IgA and IgE antibodies are expressed. T_H2 cells have various effects on macrophages and they activate B cells to produce neutralizing antibodies. (Janeway et al., 2005) T_H2 cells play a role in the defense against certain helminthes and other extracellular parasites. Moreover, T_H2 cells

activate mast cells and eosinophils and their cytokines induce B lymphocytes to switch to IgE-producing cells. (Rautajoki et al., 2008)

Several studies have linked IL-4 overexpression to T_H2-related immunological disorders. Allergic asthma is a chronic inflammatory disease connected to accumulation of T_H2 cells, eosinophils and mast cells to asthmatic lungs. Increased IgE levels and IL-4 expression are also observed during allergic disorders. (Oboki et al., 2008) In addition, IL-4 mRNA expression is noticed to increase in patients with food allergy compared to healthy controls and the IL-4 transcripts were increased in caecal mucosa of the patients (Coëffier et al., 2005).

2.1.2.4. T_H17 cells in tissue inflammation and autoimmune diseases

IL-17 (also known as IL-17A) is produced by T_H17 cells and it is associated with host defense against infectious agents, by recruiting neutrophils and macrophages to infected tissues during inflammatory response (Dong, 2008). Many autoimmune diseases, such as murine arthritis and encephalomyelitis, were previously connected to T_H1 pathway, but recent gene-deficient mice models indicate, that T_H17 cells are responsible for these diseases. (Oboki et al., 2008) IL-17-deficient mice have decreased antigen-specific T cell activation and antibody production in autoimmune and allergy disease models (Nakae et al., 2002; Nakae et al., 2003). T_H17 cells affect the pathogenesis of several autoimmune diseases by inducing cytokines and chemokines that promote chemoattraction of inflammatory cells (Rabin & Levison, 2008). Actually, the increased IL-17 levels have been detected in patients with various autoimmune diseases such as systemic lupus erythematosus, multiple sclerosis, inflammatory colitis and rheumatoid arthisis (Kurts, 2008). The role of IL-17 may be either pathogenic or protective towards immunological diseases, for instance, IL-17 is considered to promote encephalomyelitis, but it has protective effects, for example, against acute colitis (Dong, 2008).

Allergic asthma is usually connected to T_H2 cells but there are some suggestions, that T_H17 pathway may promote non-T_H2-type asthma (Oboki et al., 2008). It is also suggested that T_H17 cell infiltration in asthmatic airways links T cell activity with neurophilic inflammation in asthma, because IL-17 levels are significantly elevated in asthmatic patients compared to healthy controls (Bullens et al., 2006).

2.1.3. Regulatory mechanisms of the immune system

The balance between immunity and tolerance is maintained by T_{reg} cells that include T_R1 cells and nT_{reg} cells (Figure 1) (Cools et al., 2007). T_{reg} cells play beneficial roles by diminishing collateral tissue damage in several examples of viral, bacterial and parasitic infections (Rouse, 2007). T_{reg} cells control the immune responses and silence self-reactive T cells and they need a TCR to trigger their suppressive function. T_R1 cells mediate their suppressive activity by producing soluble factors, mainly cytokine IL-10, while nT_{reg} cells act via direct cell-cell contact-dependent stimulation between suppressor and effector cells. (Cools et al., 2007)

As mentioned, T_R1 cells express IL-10 and some pathogens can induce this gene expression. T_R1 cells may also limit collateral tissue damage associated with the immune response. (Rouse, 2007) Moreover, T_R1 cells may play a role in allergic disorders functioning by producing IL-10 as a response to allergens (Akdis, 2006).

nT_{reg} cells develop in the thymus. Their TCR repertoire is mainly self-reactive and they are differentiated from $CD4^+$ and $CD25^+$ cells. nT_{reg} cells express Foxp3 that is a forkhead box transcription factor and it is involved in the differentiation of T cells into a regulatory function. A healthy individual does not normally develop tissue destructive autoimmunity because of the presence of nT_{reg} cells, but without normal Foxp3 control multisystem autoimmunity occurs. Usually, autoimmunity is associated with situations, where global defects of nT_{reg} cells are not present. *In vitro* studies have revealed that nT_{reg} cells with Foxp3 can exert suppressive effects against multiple cell types involved in immunity and inflammation. These effects include, for instance, the effector and memory function of CD4+ and CD8+ cells, the inhibition of proliferation, immunoglobulin production and class switching of B cells, the inhibition of NK cell cytotoxicity as well as effects on the function and survival of neutrophils. However, it is still unsure how nT_{reg} cells exert their inhibitory effect *in vivo* and almost certainly multiple mechanisms could be possible. It may be possible to manipulate nT_{reg} cells to treat immunological diseases, for example, diabetes may be a candidate for nT_{reg} manipulation therapy. (Rouse, 2007)

2.1.4. Failures of immune regulation: Allergies and autoimmune diseases

Disorders in the balance between T_H1 and T_H2 cells lead to excessive T_H1 cell or T_H2 cell activation. Accumulation of T_H1 cells causes autoimmune diseases and accumulation of T_H2 cells induces allergic disorders. (Oboki et al., 2008) T_H17 cells may also play a role in development of autoimmune diseases (Dong, 2008).

Autoimmune responses resemble normal immune responses, but the reaction pathway is activated by self-antigens instead of foreign antigens. The main purpose of the T_H1 cells is to make effective responses against pathogens by destroying the antigens via cellular immunity. Moreover, in some cases the body can produce auto-antibodies to mark the own cells for destruction. So, a critical function of immune system is to discriminate self from non-self and this function is disturbed in autoimmune diseases. Autoimmune reactions can be divided into organ-specific and systemic, for example, only pancreatic β-cells are destroyed in organ-specific autoimmune reaction diagnosed as type 1 diabetes. (Janeway et al., 2005)

Allergic reactions occur when an individual, who has produced IgE antibody in response to an innocuous antigen (allergen), encounters the same allergen again. Allergy is also termed hypersensitivity reaction where harmful immune responses cause tissue injury and allergic disease. Common allergens include drugs, animal hair, insect bites, pollens and food allergens such as peanuts, tree nuts, fish and milk. (Janeway et al., 2005) Allergic disorders affect approximately 30% of the population in developed countries and they are both genetically and environmentally influenced multifactorially regulated diseases. Allergic disorders are associated with chronic inflammation characterized by influx of a large number of eosinophils, accumulation of mast cells in the lesions and increased IgE production. (Oboki et al., 2008) Allergic rhinitis is a common allergic disease affecting approximately 10-12% of the world's population. The symptoms, that are rhinorrhea, nasal obstruction, nasal itching and sneezing, are reversible and caused spontaneously by exposure to allergens. IgE-mediated immunologic mechanisms are known to play a key role leading to the release of mediators, such as histamine, that induce allergic symptoms. (Wang, 2005)

2.1.4.1. The effect of genetic and environmental factors on immunological diseases

The incidence of many autoimmune and allergic diseases has increased in developed countries during past three decades. This increase has happened in asthma, rhinitis and atopic dermatitis which represent allergic diseases as well as in celiac disease, multiple sclerosis and type 1 diabetes mellitus, which represent autoimmune diseases. Several studies have found that populations with a low socioeconomic status have a lower frequency of these diseases compared to countries with a high socioeconomic status. It has also been noticed that the incidences of multiple sclerosis, type 1 diabetes and asthma are increasing among populations which migrate from a low-incidence country to a high-incidence country. (Bach, 2002) One explanation for the increasing prevalence of allergy is the hygiene hypothesis. A number of epidemiologic studies have supported the idea that T_H1 responses induced by microbial stimulations can counterbalance allergen-induced T_H2 responses. However, also other environmental changes such as increased air pollution and changed lifestyle may contribute to increased risk of allergic sensitization. (Wang, 2005)

When type 1 diabetes, celiac disease, thyroid autoimmunity and allergic sensitization were studied in two neighboring populations, which live in completely different socioeconomic environments (Finland and Karelian Republic of Russia), it was found that all these immune-mediated disorders were several times more common in Finland. Finland was also characterized by much lower frequency of microbial infections such as helicobacteria and hepatitis A. Moreover, infections were associated with protection against allergic sensitization in Russian Karelia. HLA risk genes for autoimmune diseases did not markedly differ between the two populations. Collectively, these studies support the concept of hygiene hypothesis and the role of childhood infections in the regulation of immune system. They also suggest that the immune pathogenesis of allergies and autoimmune diseases may be partly regulated by common mechanisms. (Kondrashova et al., 2005, Kondrashova et al., 2007, Kondrashova et al., 2008a, Kondrashova et al., 2008b and Seiskari et al., 2007)

Less than 50% of identical twins with immune-mediated disease have a healthy twin being thus discordant for the disease. This speaks for a genetic component in the pathogenesis as the incidence rate of identical twins exceeds the normal population level incidence. On the other hand, the lack of 100% concordance suggests that environmental factors are also important. (Beyan et al., 2003) In some diseases the risk genes have been identified and their polymorphism correlates with the

increased risk of the disease (such as HLA, CTLA4, insulin, MDA5 and PTPN22 genes in type 1 diabetes) (Näntö-Salonen et al., 2009).

2.1.4.2. Type 1 diabetes

Type 1 diabetes occurs in childhood and it is considered to be a chronic immune-mediated disease with a subclinical prodrome of variable duration. Destruction of insulin-producing pancreatic β-cells may lead to disease manifestation within few months in infants and young children, whereas the duration can be much longer, even more than 10 years, in some individuals. The appearance of diabetes-associated autoantibodies, such as classic islet cell antibodies, insulin autoantibodies, autoantibodies to the 65-kDA isoform of GAD and the tyrosine phosphatase-related IA2 molecule, is the first detectable sign of emerging β-cell autoimmunity. Positivity to three to four autoantibodies is associated with clearly increased risk to develop type 1 diabetes with probability of 60-100% during the next 5-10 years. (Knip et al., 2005)

The incidence of childhood diabetes is increasing worldwide and the increase is annually 3% per year. Type 1 diabetes is a result of T cell-mediated autoimmune process directed against the insulin producing β-cells of the pancreas, whereas type 2 diabetes is not an autoimmune disease and it results from a combination of insulin resistance and disturbed function of pancreatic β-cells. 60-80% of β-cells must be destroyed in type 1 diabetes before clinical symptoms such as polyuria, polydipsia, weight loss and ketosis occur. Microvascular and macrovascular complications are also related to type 1 diabetes and they account for most of the increased morbidity and mortality of the disease. (van der Werf et al., 2007)

In the United States diabetes mellitus occurs at an incidence of 12 to 15 cases per 100 000 persons per year and the worldwide incidence ranges from 3-30 cases per 100 000 persons per year (Richman et al., 2002). Finland has the highest recorded incidence of childhood diabetes (Kupila et al., 2001) being currently more than 60/100 000 individuals per year.

The genetic risk to type 1 diabetes is mainly conferred by particular HLA haplotypes such as HLA-DR and DQ (Näntö-Salonen et al., 2009). Only a relative small proportion that is less than 10% of genetically susceptible individuals progress a clinical disease indicating, that environmental factors have a significant role in type 1 diabetes development (Knip et al., 2005). It is suggested, that there

is a connection between childhood enterovirus infections and type 1 diabetes development (Richman et al., 2002). However, cow's milk protein, nitrites and lack of vitamin D have also been associated with type 1 diabetes development (Tauriainen et al., 2005).

2.2. An insight into enteroviruses

Enteroviruses belong to the picornavirus family and they are non-enveloped positive-strand RNA viruses. They are small, approximately 27-30 nm in diameter, consisting of a simple virus capsid and a single strand of positive-sense RNA. The viral capsid is formed from 60 repeating protomeric units of an icosahedron that is constructed from four viral proteins VP1 to VP4. Enteroviruses replicate in human gastroenteric tract where they usually bind to specific receptors of enterocytes. (Richman et al., 2002) More than 100 different serotypes of human enteroviruses are known, including 3 polioviruses, 23 Coxsackie A serotypes, 6 Coxsackie B serotypes, 28 echovirus serotypes and several newer numbered serotypes. Recently, rhinoviruses were also included into the enterovirus family. Enterovirus infections are mostly subclinical or manifest with only mild respiratory symptoms. However, they can also lead to severe diseases such as paralysis, meningitis, myocarditis and systemic infections in newborns. (Tauriainen et al., 2005)

The nonpolio enteroviruses are estimated to cause 10 to 15 million symptomatic infections in the United States per year while the polioviruses are well controlled in developed countries due to efficient vaccination. Enterovirus infections show a clear seasonal pattern and they occur typically during periods of warm weather, especially in autumn and among children. The virus transmission can happen during direct person-to-person contact, houseflies, waste water and sewage. The infection incidence is higher in children but the severity of infection as a function of age varies according to disease and serotype. (Richman et al., 2002)

Enteroviruses cause a wide variety of severe diseases and symptoms. Neurologic illnesses caused by enteroviruses include poliomyelitis, aseptic meningitis and encephalitis. Neonatal sepsis is an example of the neonate or young infant infection. Respiratory illnesses include, for instance, herpangina, pleurodynia and hand-foot-and-mouth disease. Also enterovirus-mediated cardiovascular illnesses exist, such as acute myocardis. (Richman et al., 2002) Despite severe diseases, most of the symptoms are mild (Viskari et al., 2004).

2.2.1. The role of enteroviruses in type 1 diabetes

Enterovirus infections are among the most likely environmental candidates to cause type 1 diabetes (Viskari et al., 2004). The relationship between enteroviruses and type 1 diabetes was reported first time 40 years ago when Coxsackievirus B antibodies were found more frequently with diabetic patients than within healthy controls (Gamble et al., 1969). It is suggested that enteroviruses can trigger and modulate type 1 diabetes development via different mechanisms, including direct β-cell lysis caused by viral infection, bystander activation of autoreactive T cells, loss of regulatory T cells and molecular mimicry. The process is affected by multiple mechanisms and precipitating factors. Important precipitating factors are nature of the virus, viral load and immunological status of the host. (van der Werf et al., 2007) The ability of the enterovirus to cause β-cell damage may be determined only by a few or even one point mutation that have an effect on, for instance, viral tropism which is the ability to infect certain cell types (Tauriainen et al., 2005).

Enterovirus infections have been diagnosed more frequently in type 1 diabetic patients than in the healthy population. Enteroviruses have also been found in the pancreas of the patients and ongoing infections have been detected on their intestinal mucosa, where the primary replication of the virus occurs. (Oikarinen et al., 2007) Enterovirus infections are less frequent in countries with high diabetes incidence compared to low incidence countries suggesting that there is an inverse correlation between type 1 diabetes and enterovirus infections in the background population. As an explanation, the enterovirus infections may be more severe as the immune protection, especially that provided by maternal antibodies for the newborns, has decreased in countries with a low frequency of infections. (Viskari et al., 2004)

A vaccine is already available to polioviruses 1-3, which cause severe paralytic diseases. If diabetogenic enteroviruses belong to certain serotypes, as expected from other enterovirus diseases like polio, it may be possible to design an enterovirus vaccine which could prevent from diabetes. (Tauriainen et al., 2005)

2.3. Analysis of cytokine expression with real-time PCR

There are currently five main chemistries available for the detection of PCR (polymerase chain reaction) product with real-time PCR which are based on fluorescence dyes. These methods include DNA binding fluorophores, 5' endonuclease, adjacent linear and hairpin oligoprobes and self-fluorescing amplicons. (Mackay et al., 2002) In this study the real-time PCR method with SYBR Green chemistry based on DNA binding fluorophores was used for quantification of cytokine expression levels from human white blood cells. Therefore, this chapter introduces the common concept of the real-time PCR especially with SYBR Green chemistry.

2.3.1. Principle of quantitative real-time PCR

Any nucleic acid present in a complex sample can be amplified in a cyclic process called PCR to generate a large number of identical copies that can readily be analyzed. Real-time PCR enables simultaneous amplification and detection of specific DNA sequences. The amount of product formed is monitored during the reaction by monitoring the fluorescence dyes or probes introduced into the reaction that is proportional to the amount of product formed. Moreover, the number of amplification cycles required to obtain a particular amount of DNA molecules is registered. Typically the real-time PCR is used in a pathogen detection, gene expression analysis, single nucleotide polymorphism analysis and analysis of chromosome aberrations. (Kubista et al., 2006)

PCR is performed on a DNA template with two oligonucleotide primers that flank the DNA sequence to be amplified, dNTPs, which are the four nucleotide triphosphates, a heat-stable polymerase and magnesium ions. These elements together form the reaction mixture. The reaction is executed by temperature cycling, where a high temperature, about 95 ºC, is applied to separate the strands of the double helical DNA. Then temperature is lowered to let the primers anneal with the template approximately at 60 ºC. Finally, the temperature is set around 72 ºC, which is optimum for the polymerase. The polymerase extends the primers by incorporating the dNTPs. The annealing temperature depends on the primers and theoretically it should be few degrees below their melting temperature. (Kubista et al., 2006)

Real-time PCR needs a fluorescent reporter that binds to the PCR product and reports its presence by fluorescence. Several probes and dyes are available commercially. During the initial cycles the signal is weak and cannot be distinguished from the background, but when the amount of PCR product accumulates, the fluorescence signal increases exponentially above the threshold level. Thereafter the signal level saturates and comes to plateau phase due to the reaction running out of some critical component like primers, polymerases or the dNTPs. Typically real-time PCR response curves saturate at the same level, but the interesting part is the growth phase of the reaction, which reflects the difference in the initial amounts of template molecules. (Kubista et al., 2006) Fluorescence values are recorded during every cycle. The more target template is present at the beginning of the reaction, the fewer number of cycles it takes to reach the point in which the fluorescent signal is first recorded as statistically significant above background. This CT (cycle threshold) point describes the number of the cycles and it occurs always during the exponential phase of amplification (Figure 2). Therefore, quantification is not affected by any reaction components becoming limited in the plateau phase. (Bustin, 2000) Figures 2 and 3 represent the phenomenon described above. Rn axis is logarithmic meaning that the amplification happens exponentially. This exponential growth is demonstrated as a function of the number of the cycles.

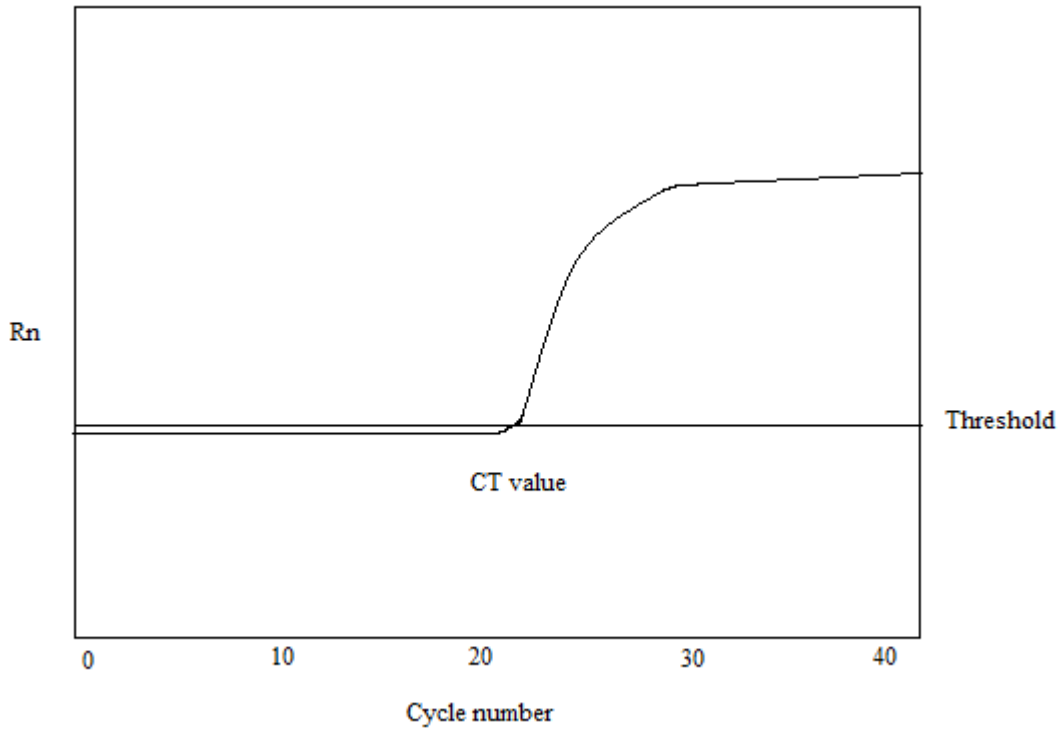

Figure 2. Location of the CT point in the real-time PCR amplification plot.

After the real-time PCR run with Applied Biosystems HT7900 instrument with SYBR Green chemistry amplification plot and dissociation curve are available. Figure 3 demonstrates the amplification plot for three samples from which the amount IFN-γ mRNA is measured and the variation of CT points between the three samples is visually detectable.

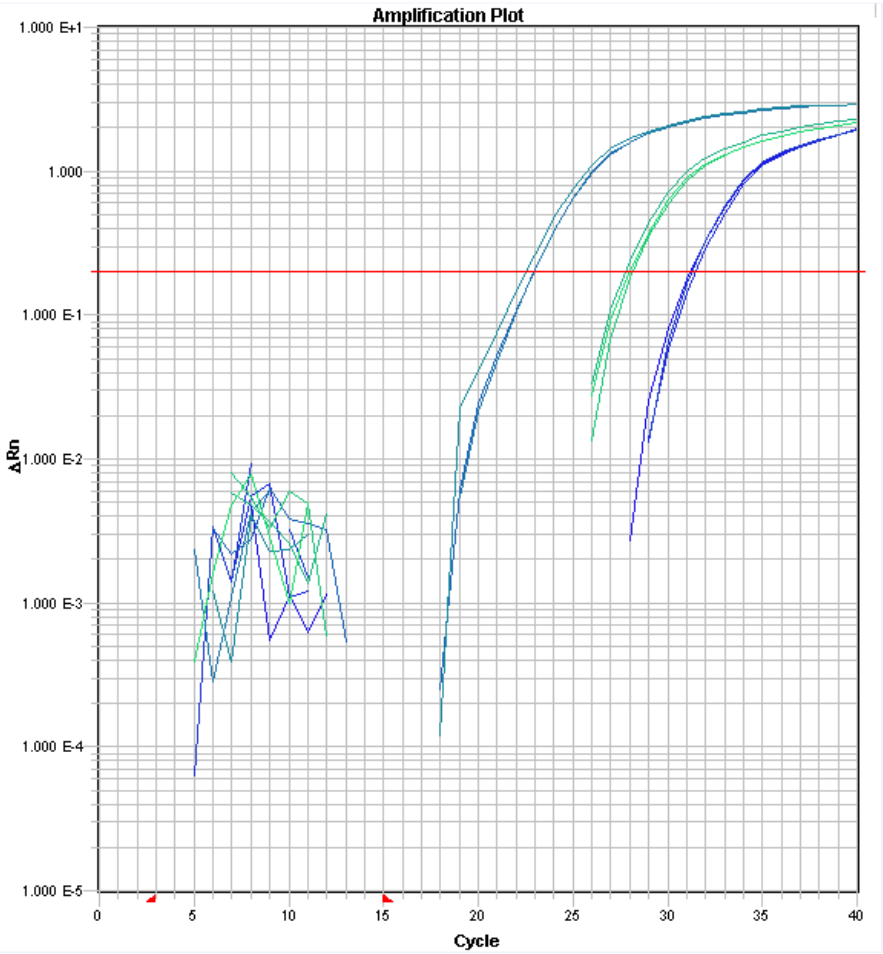

Figure 3. Amplification plot for the analysis of IFN-γ gene expression. CT values (22.8, 27.9 and 31.3 in order from left to right) are represented for three samples. Primer-dimer formation is represented on the left where the lines follow no clear pattern.

Dissociation curve for the same three samples is shown in Figure 4 where only one melting spike is observed reflecting that only one reaction product has been formed. The melting point locates in the middle of the melting spike as represented in Figure 4 with melting temperature 78.5 °C. More information about dissociation curve is offered in Chapter 2.3.3.

Nowadays, many instruments are available for quantitative real-time PCR including, for example, ABI Prism 7700 (Perkin Elmer-Applied Biosystems) and HT7900 (Applied Biosystems) (Bustin, 2000).

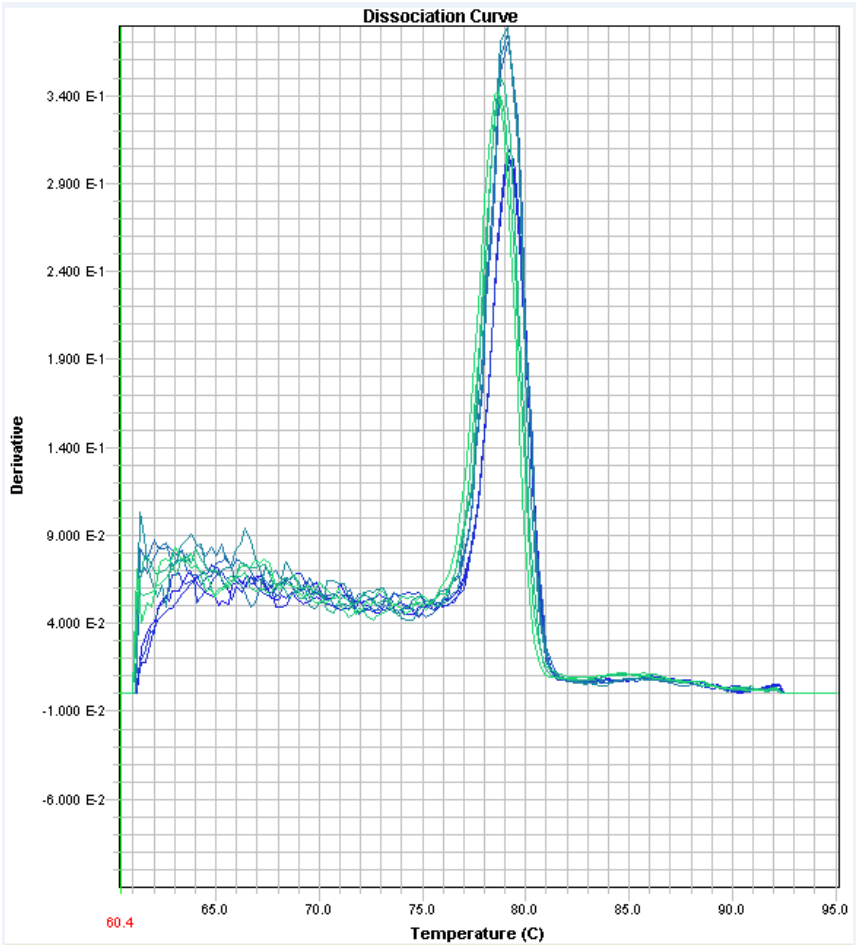

Figure 4. Dissociation curves for three samples with different CT values. Only one melting spike is observed reflecting melting temperature 78.5 °C.

2.3.2. Real-time PCR with SYBR Green chemistry

Both sequence specific probes and non-specific labels are available as fluorescence reporters. Asymmetric cyanine dyes, such as a sequence non-specific dye SYBR Green, have become more popular recently. Asymmetric cyanines have two aromatic rings containing nitrogen from which one is positively charged and the rings are connected by a methine bridge. These dyes have no detectable fluorescence when they are free in solution, since vibrations engaging both aromatic systems dissociates to the surrounding solvent. However, the dyes become brightly fluorescent when binding to DNA minor groove, because the rotation around the methine bond is restricted. During the real-time PCR assay the fluorescence of these dyes increases with the amount of double stranded DNA product formed. The presence of the same amount of double-stranded DNA gives rise to the same fluorescence every time. (Kubista et al., 2006) SYBR Green absorbs light with a

wavelength of 480 nm and emits light with a wavelength of 520 nm and the emission of fluorescence is 1000-folds greater when the dye is bound to DNA compared to the situation when it is free in the solution. (Valasek & Repa, 2005)

2.3.3. Common error sources and drawbacks of real-time PCR

One possible error source is due to 2–4 consecutive guanine repeats which may fold the template into a tetraplex structure, which is exceedingly stable and cannot be transcribed by the polymerase. On the other hand, if the primer contains the tetraplex structure, it is unable to bind to the template. Self-complementary regions in the template or in the primers can also cause problems by folding into hair-pins and other structures that may interfere with the extension. Complementarity between the primers, especially in their 3'-ends, causes complications by forming aberrant PCR products called primer–dimers. (Kubista et al., 2006) The melting curve analysis is represented in Figure 5 and the primer-dimer spike occurs in lower melting temperature than the PCR product spike.

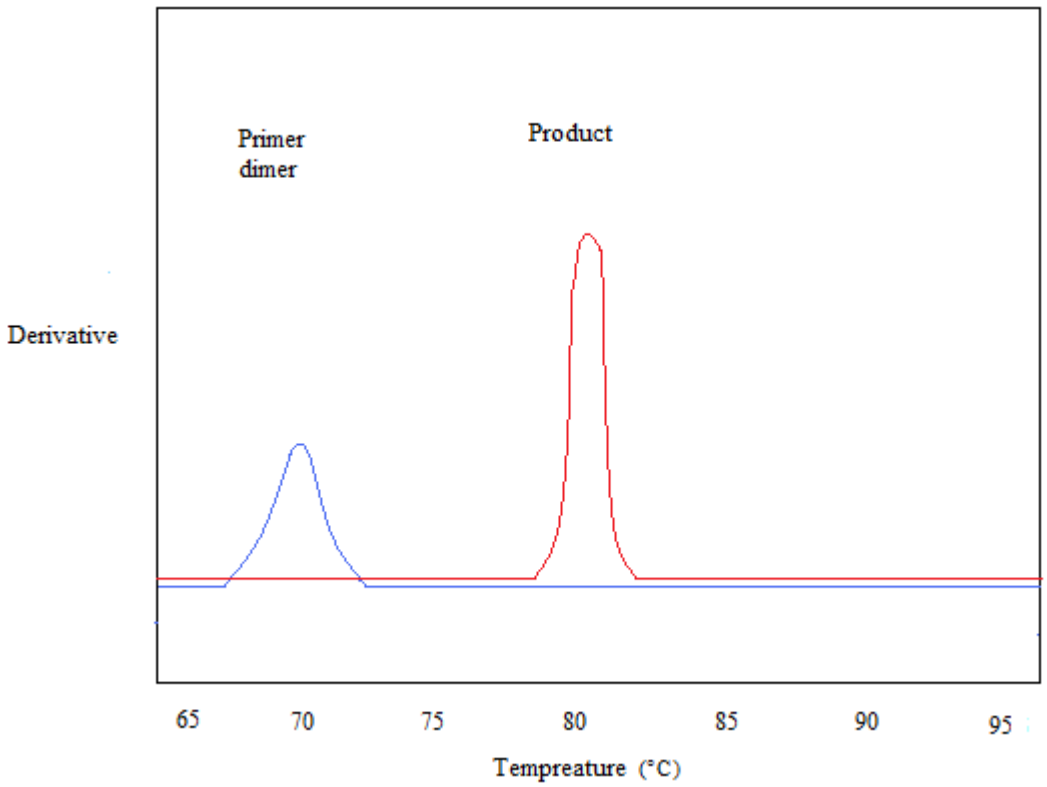

Figure 5. Real-time PCR dissociation curve. The figure shows the derivative as a function of temperature (°C). The dissociation curve of the PCR product is described as red and the undesirable primer-dimer dissociation curve as blue.

Avoiding the formation of primer–dimer products is very important for quantitative PCR analysis of samples that contain only few target molecules, since the PCR of the target and the PCR of the primer–dimers compete. The primer–dimer formation can be controlled by doing melting curve analysis after completing the real-time PCR. In melting curve analysis the temperature is gradually increased and the fluorescence signal is measured as a function of temperature. The fluorescence decreases gradually with increasing temperature due to increased thermal motion that allows more internal rotation in the bound dye. When the temperature, at which the double stranded DNA strands are separated, is reached, the dye comes off and the fluorescence drops abruptly. This temperature is referred to as the melting temperature (T_m) and it is determined as the maximum of the negative first derivative of the melting curve. Since the primer–dimer products are typically shorter than the target product, they can be recognized from the melting curve analysis, because they have a lower melting temperature. (Kubista et al., 2006)

One drawback of the real-time PCR with SYBR Green chemistry is that multiple dye molecules bind to a single amplified molecule and, consequently, the amount of signal generated after irradiation is dependent on the mass of double-stranded DNA produced in the reaction. Therefore, assuming that the amplification efficiencies do not differ, the amplification of a longer product will generate more intense signal than a shorter one. This drawback can be avoided if specific probes are used to detect amplified DNA. In such case, similar signal of fluorogenic probes is observed for each amplified molecule, regardless of its length. (Bustin, 2000)

2.3.4. Normalization and Pfaffl equation for relative quantification in real-time PCR

Normalization is needed for minimizing the errors of sample-to-sample variations and it can be corrected by using internal reference against the target sample (Bustin, 2000). The Pfaffl equation shows a mathematical model to determine the relative expression ratio in the real-time PCR based on the relative expression of a target gene versus a reference gene to investigate physiological changes in the gene expression. The target gene is normalized with the endogenous standard to compensate inter-PCR variations between the runs. The reference gene can be some of the housekeeping genes that are present in all nucleated cell types, since they are necessary for cell survival, and the gene expression is considered to be stable in various tissues. The Pfaffl equation is represented below,

$$ratio = \frac{(E_{t\ \arg\ et})^{\Delta CT_{t\arg et}(control-sample)}}{(E_{ref})^{\Delta CT_{ref}(control-sample)}}$$

where E_{target} is the real-time PCR efficiency of target gene transcript, E_{ref} is the real-time PCR efficiency of a reference gene transcript, ΔCT_{target} is the CT deviation observed in target gene expression (CT values) between control sample and analytical sample and ΔCT_{ref} is the CT deviation in reference gene expression between control sample and analytical sample. (Pfaffl, 2001)

The efficiency of the PCR assay can be estimated with a standard curve based on dilution series of a standard sample. However, biological samples are complex and may contain inhibitory substances that are not present in the standard sample. (Kubista et al., 2006) The corresponding real-time PCR efficiencies (E) are calculated according to the equation $E = 10^{[-1/slope]}$ where 10 is the dilution coefficient and the correlation coefficient of the slope must be $r > 0.95$ (Pfaffl, 2001). In this study the dilution coefficient is 2 and thus the efficiency is calculated as $E = 2^{[-1/slope]}$.

3. AIMS OF THE RESEARCH

The aim of this study was to design primers and to optimize the real-time PCR method for three proinflammatory cytokines IFN-γ, IL-4 and IL-17. As an outcome a panel is created to study the cytokine mRNA expression of the three proinflammatory T helper cell lineages T_H1, T_H2 and T_H17 from human white blood cells with real-time PCR.

Another aim was to develop a method for the isolation of mRNA from frozen buffy-coat samples which contain white blood cells. It was recognized, that this was a challenging sample type, and the mRNA isolation from the frozen buffy-coat samples was not succeeded in previous experiments done in the Virology Research Group. In addition, there were no previous publications available on successful mRNA isolation and further analysis with real-time PCR from frozen buffy-coat samples, which have been stored for years in -70 °C freezers. Buffy-coat samples of the DIPP study have been collected since year 1994, and this aim is important for the analyses of these samples.

The final aim was to use this validated real-time PCR panel to analyze the expression of proinflammatory cytokines in mononuclear cell and buffy-coat samples taken from children participating in the DIPP study and to research the effect of enterovirus infections on the balance of immune system. The real-time PCR panel could also be used for the detection of *in vitro* stimulated expression of proinflammatory cytokines in human white blood cells.

4. METHODS

4.1. Summary of sample procedure for expression analyses

Human blood samples were obtained from healthy volunteers and from the children participating in the prospective DIPP study. White blood cells were isolated from the blood samples using two methods: mononuclear cells were isolated using commercially available blood collection tube (CPT-tube) and buffy-coat samples were prepared by centrifugation and following lysis of contaminating red blood cells using isotonic chock. The buffy-coat samples contain most of the white blood cells and platelets and are also contaminated by some erythrocytes. Therefore, they are not as pure as mononuclear cell samples making the buffy-coat samples more challenging for real-time PCR analyses. On the other hand, the buffy-coat samples are cheaper to collect as they do not require labor-intensive purification process.

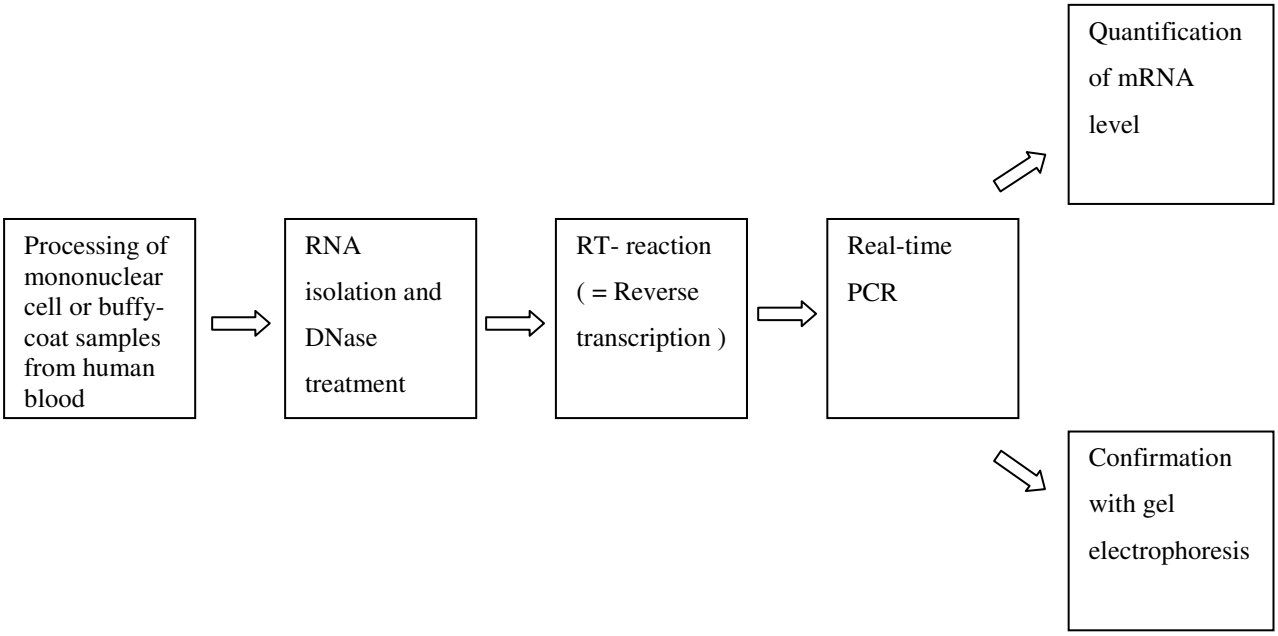

Figure 6. Different steps of the sample procedure for expression analyses with real-time PCR.

The mRNA analysis with real-time PCR included several steps (Figure 6), starting from the processing of the mononuclear cell or buffy-coat samples and followed by mRNA isolation with DNase treatment. Several methods were tested to optimize mRNA purification from buffy-coat samples. Then, RNA was transcripted with RT-reaction into cDNA, which contains the mRNA information of the cytokine expression from human white blood cells. cDNA samples were

analyzed with real-time PCR to quantify absolute or relative cytokine mRNA levels. The relative gene expression was calculated using Pfaffl equation. Amplification of target cDNA was confirmed with agarose gel electrophoresis.

4.2. DIPP study

DIPP (Diabetes Prediction and Prevention) study is an effort aiming at prediction and search for means to delay and prevent type 1 diabetes in a large population-based cohort of children in Finland (Kupila et al., 2001). The DIPP study was started in 1994 and babies from general population and their older siblings were screened for HLA-DQB1 alleles that are associated in susceptibility of type 1 diabetes. Individuals of this genotype develop type 1 diabetes before age of 15 years with an average risk of 3-8%. The protocols of DIPP study have been approved by the local institutional review boards and ethical committees. (Näntö-Salonen et al., 2009) In other words, DIPP study is based on the screening of newborns for increased genetic risk for type 1 diabetes and the prospective follow-up of children who carry increased genetic risk. Overall 11,000 newborns are screened annually for HLA-risk alleles. The purpose of the project is to study the risk factors of type 1 diabetes in order to develop new treatment and prevention methods. The study is carried out in Finland in three locations in the cities of Turku, Tampere and Oulu. Children with increased risk are recruited to a follow-up study in which they are seen at 3-6 months intervals for 2 years and at 6-12 months intervals thereafter. A blood sample is taken in every visit. To year 2008, over 8500 children carrying increased genetic risk for type 1 diabetes have participated in the follow-up and over 110 of them have progressed to clinical diabetes. More information about the DIPP study is available online (http://research.utu.fi/dipp/index.php?page=MAIN&lang=EN&city=TURKU).

4.3. Sample processing

The blood samples obtained from healthy volunteers and from the DIPP children are processed to isolate white blood cells using two different procedures to purify either mononuclear cells or buffy-coat. First, the processing of the mononuclear cells, and second, the processing of buffy-coat are described. Moreover, there are two different ways for buffy-coat sample processing and the technique used depends on the processing year. Sample processing method used before year 2001

differs from technique used after year 2001. The most critical distinction is the varying final sample volume of the buffy-coat samples processed in different ways.

4.3.1. Purification of the mononuclear cells

The blood samples were processed using a special 4ml or 8ml CPT sodium-nitrate tube (DB, USA), which allows purification of mononuclear cells by a single centrifugation step at 1700rpm for 15 minutes. The mononuclear cell layer containing lymphocytes and monocytes was pipetted together with a small amount of autologous plasma into two 1.2ml cryotubes which were snap-frozen in liquid nitrogen for one day and moved then to -70°C for long-term storage. The final volume of the samples was approximately 100-200µl. The mononuclear cell samples were processed in the Virology Research laboratory at the University of Tampere.

4.3.2. Purification of the buffy-coat

Blood sample was drawn into a standard sodium-nitrate tube. After centrifugation at 1700rpm at room temperature, the red blood cells compose the bottom layer and plasma forms the top layer, when white blood cells form a white intermediated layer on the top of the red blood cells. This white blood cell layer contains all types of white blood cells and is called buffy-coat. In the next step, the buffy-coat was gently removed by pipet into another tube. Since this buffy-coat contains contaminating red-blood cells, which can be harmful in molecular assays, red-cell lysis was next carried out using osmotic chock. In this lysis-step distilled water (4°C) was added on the buffy-coat sample filling about ¾ of the total 10ml volume of the tube. The sample was mixed by turning it up and down and incubated for 30 seconds at room temperature to lyse the red blood cells. After this the osmolarity was restored to physiological conditions by adding 4°C 3.6 % NaCl. Next the tube was centrifuged for 5 minutes and supernatant was removed. The pellet containing the white blood cells was diluted into 100µl of distillated water and snap-frozen in liquid nitrogen followed by long-term storage at -70°C. The final volume of the samples was around 100-200µl with this technique used after year 2001. Before year 2001 the pellet was diluted into 300-500µl of distillated water before transmitting it into a new tube. Therefore, there was a wide variation in the final volume of the buffy-coat samples ranging from 200µl to 1000µl. The differences in final sample volumes have an effect on RNA isolation methods and protocol modifications as shown in Table 1.

4.4. RNA isolation

RNA isolation from human mononuclear cell samples was carried out using Qiagen RNeasy® Mini Kit with Animal Cells Spin protocol. The same kit with modified protocols was also used for RNA isolation from buffy-coat samples. RNA isolation from buffy-coat samples was also tested with Qiagen Oligotex® Direct mRNA Mini Kit with Animal Cells protocol and Qiagen AllPrep® DNA/RNA/Protein Mini Kit with Cells protocol. The Oligotex® kit protocol is available in Qiagen Oligotex® Handbook (Second Edition, May 2002) and the AllPrep protocol in Qiagen AllPrep® DNA/RNA/Protein Mini Handbook (December 2007). The RNA isolation protocol of Allprep® is similar to the protocol of RNeasy® Mini Kit, but there are also additional protocols for DNA and protein purification.

4.4.1. RNA isolation from the mononuclear cell samples with Qiagen RNeasy® Mini Kit

Total RNA was isolated with Qiagen RNeasy® Mini Kit from the human mononuclear cell samples. Qiagen RNeasy® Mini Kit is designed to purify total RNA from animal cells, animal tissues and yeasts. RNeasy® Mini Kit combines the selective binding properties of a silica-based membrane and the speed of the microspin technology. The kit contains all the reagents needed in the total RNA purification except 70% ethanol. For human mononuclear cells Animal Cells Spin protocol was used and the procedure included the following three separate steps using spin columns: lysis, binding of the RNA to membrane and elution of the RNA.

The human mononuclear cell samples were stored at -70ºC. The frozen samples were disrupted by adding 350µl or 600µl RLT lysis buffer directly to frozen sample and the samples were melted with the lysis buffer for 10 minutes at room temperature. The amount of RLT buffer depended on the cell number of the sample. The lysate was homogenized with a QIAshredder spin column, after which the lysate was moved directly to the QIAshredder spin column placed in a 2ml collection tube and centrifuged at full speed (13,200 rpm) for 2 minutes. After centrifugation one volume (about 700µl) of 70 % ethanol was mixed to the homogenized lysate and the sample was transferred to an RNeasy spin column placed in a 2ml collection tube and centrifuged at 10.000rpm for 15 seconds. The RNA was bound to the spin column and the flow-through was discarded.

RNeasy technology removes efficiently most of the DNA. However, further DNA removal by DNase treatment using QIAGENin Rnase-Free Dnase Set was necessary for applications that were sensitive to very small amounts of DNA such as the real-time PCR. 350µl Buffer RW1 was added to the RNeasy spin column and centrifuged at 10,000rpm for 15 seconds and the flow-through was discarded. 10µl DNase1-solution was mixed with 70µl RDD buffer per one sample and 80µl of this DNase1 incubation mix was added directly to the RNeasy spin column and incubated at 20-30ºC for 15 minutes. Again, 350µl Buffer RW1 was added to the RNeasy spin column and centrifuged at 10,000rpm for 15 seconds and the flow-through was discarded. If DNase treatment was skipped, then 700µl RW1 buffer was added to RNeasy spin column and centrifuged at 10,000rpm for 15 seconds and the flow-through was discarded.

In both the DNase treatment protocol and the protocol without DNase treatment the next step was washing the column with 500µl RPE buffer and centrifugation at 10,000rpm for 15 seconds. Then, the wash was repeated with 2 minutes centrifugation. The flow-through was discarded after both centrifugations. Finally, the RNA was eluted to RNase-free water from the RNeasy spin column, which was placed in a new 1.5ml collection tube. 50µl RNase-free water was added directly to the spin column membrane and centrifuged at 10,000rpm for 1 minute. The flow-through contained the RNA. (Qiagen RNeasy® Mini Handbook, April 2006).

As an assumption the DNAse treatment was carried out to all samples and exceptions to this statement are separately mentioned in the text.

4.4.2. RNA isolation from the buffy-coat samples with Qiagen RNeasy® Mini Kit

RNA isolation from frozen buffy-coat samples was tested with Qiagen RNeasy® Mini Kit using modified Animal Cells Spin protocols (Modifications 1-4) as described below and summarized in Table 1. The base of these modified protocols was similar to the RNA isolation protocol represented in Chapter 4.4.1. for mononuclear cell samples. Modifications 1 and 2 focus on the buffy-coat samples having a final volume of 200-1000µl, while modification 3 and 4 consider the samples with a final volume of 100-200µl. The variation in sample volumes was explained in Chapter 4.3.2. Again, the DNAse treatment was carried out for all samples and exceptions to this rule are separately mentioned.

Table 1. Summary of the modifications 1-4 for RNA isolation with Qiagen RNeasy® Mini Kit.

RNA isolation method	Sample volume (µl)	RLT (µl)	Homogenization	Ethanol added to lysate
Modification 1	200-1000	600	QIAShredders	96-100% ethanol
Modification 2	200-1000	600	20G needle and syringe	96-100% ethanol
Modification 3	100-200	900	QIAShredders	70% ethanol
Modification 4	100-200	900	20G needle and syringe	70% ethanol

In Modification 1 homogenization was carried out using QIAShredder columns. Careful vortexing was done during the cell lysis and homogenization steps. According to the original protocol, one volume (one volume = 200-1000µl buffy-coat sample + 600µl RLT lysis buffer) of 70% ethanol should be mixed to the cell lysate during homogenization. However, for these samples, which were stored in a large 200-1000µl volume of distilled water, one volume of 96-100% ethanol was mixed to the lysate to avoid dilution of the samples.

Modification 2 was also designed for the buffy-coat samples that have the final volume of 200-1000µl. Homogenization was carried out using 20G needle and syringe by drawing the sample up and down inside the needle and the syringe. One volume of 96-100% ethanol was added to the lysate. More information about the homogenization step in Animal Cells Spin protocol is available in Qiagen RNeasy® Mini Handbook (April 2006).

Modification 3 was used for the buffy-coat samples having a final volume of 100-200µl. A larger volume (900µl) of RLT cell lysis buffer was used instead of the standard volume (600µl) of RLT buffer. QIAshredders were used for the homogenization and one volume (1 volume = 100-200µl buffy-coat sample + 900µl RLT lysis buffer) of 70% ethanol was added to the lysate.

Modification 4 also deals with samples having the final volume of 100-200µl. The protocol was similar to Modification 3, but the homogenization is carried out with 20G syringe and needle.

4.5. RT-reaction

RT-reaction (reverse transcriptase reaction) was used for the reverse transcription of the extracted RNA to cDNA prior to the real-time PCR. The RT-reaction was carried out using random primers according to the protocol designed and used by the Professor Hyöty's research group at the Virology Laboratory in the University of Tampere. First, the RNA sample and random hexamers

were mixed and incubated at +70ºC for 5 minutes. Then, the sample was moved on ice for cooling, and spinned down to the bottom of the tube. One portion of the RT-reaction mixture, which was needed for the processing of one RNA sample, is represented below in Table 2. RT-reaction mixture was prepared by mixing together water, 10mM dNTP, M-MLV RT 5xBuffer, rRNAsin and M-MLV Reverse Transcriptase-enzyme. One portion of the RT-reaction mixture was added to one RNA sample and incubated at +37ºC for one hour. Finally, the tubes containing cDNA were placed and stored at -70ºC.

Table 2. A portion of RT-reaction mixture needed for the reverse transcription of one RNA sample.

Reagent	**Volume (µl)**
RNA sample	10
Random Hexamer (TAG Copenhagen)	1,4
Aqua Sterilisara Injekt. water (or corresponding)	5,75
dNTP 10mM (Qiagen, Cat. 1005631)	1,25
M-MLV RT 5xBuffer (Promega Co., Cat. M5313)	5
rRNAsin, RNase Inhibitor 2,500u (Promega Co., Cat. N2511)	0,6
M-MLV Reverse Transcriptase–enzyme 10,000u (Promega Co., Cat. M1701)	1
Total	25

4.6. Optimization of the real-time PCR method

The real-time PCR method was optimized for three proinflammatory cytokines, IFN-γ, IL-4 and IL-17, and for one house-keeping gene TBP (TATA binding protein) by using fluorescent signal detection with Applied Biosystems 7900 HT. The procedure utilized SYBR Green chemistry of Finnzymes DyNAmo™ Flash SYBR® Green qPCR Kit. The optimization was carried out with mononuclear cell samples obtained from healthy volunteers.

4.6.1. Design of the real-time PCR primers for cytokines IFN-γ, IL-4 and IL-17

Primer pairs, each primer pair containing both forward and reverse primer as shown in Table 3, were designed for each cytokine (IFN-γ, IL-4 and IL-17). The primers were ordered from TAG Copenhagen A/S and they were designed following the instructions of Applied Biosystems Training course Basic PCR 2006. The length of the primers ranged from 20 to 24 oligonucleotides and they

did not contain complementary sequences within or between primers to prevent secondary structures and primer-dimer formation. The primer melting temperature should be 60ºC ±2ºC and the melting temperature calculations were performed using following equation: T_m = (A+T) x 2ºC + (G+C) x 4ºC. However, the calculated melting temperatures varied to some extend from the actual melting temperatures reported by the manufacturer (Table 3). Identical bases in a row were avoided and the last five nucleotides did not contain more than two G's and/or C's at the 3' end and there was no G as a first base at the 5'end. In addition, the length of the amplicons was set to be approximately equal, since the presence of the same amount of double-stranded DNA would then give rise to the same fluorescence intensity in SYBR Green chemistry (Kubista et al., 2006). Design of the primer pairs and the real-time PCR protocol for TBP was optimized previously at the Department of Virology.

Table 3. IFN-γ, IL-4, IL-17 and TBP real-time PCR primers. Primer sequences, melting temperatures and amplicon sizes are presented.

Name	Primer sequence	T_m	Amplicon size (bp)
IFNG Fwd	5'- TCT CTC GGA AAC GAT GAA ATA -3'	54.0	
IFNG Rev	5'- ACT CTC CTC TTT CCA ATT CTT -3'	54.0	202
IL-4 Fwd	5'- CTC CAA GAA CAC AAC TGA GAA -3'	55.9	
IL-4 Rev	5'- ACT CTG GTT GGC TTC CTT CA -3'	57.3	217
IL-17 Fwd*	5'- AAT CTC CAC CGC AAT GAG GA -3'	57.3	
IL-17 Rev	5'- TAG GCC ACA TGG TGG ACA AT -3'	57.3	245
TBP Fwd**	5'- CGA ATA TAA TCC CAA GCG GTT -3'	55.9	
TBP Rev**	5'- ACT TCA CAT CAC AGC TCC CC -3'	59.4	227

* (Bullens et al., 2006)
** (Isomäki et al., 2007)

Real-time PCR is very sensitive to unspecific genomic DNA amplification. Contaminating genomic DNA can be present in extracted RNA even after DNase treatment, and can lead to severe bias in assay outcomes. Therefore, special emphasis was paid on this issue and the primers were designed in such a way that they did not amplify genomic DNA. Genomic DNA amplification was prevented by designing either forward or reverse primer on the exon-exon boundary, so that only mRNA was amplified. After transcription occur mRNA splicing, where intron sequences are removed and the final mRNA contains only exon sequences (Figure 7) (Alberts et al., 2002).

The mRNA FASTA sequences of the three human cytokines IFN-γ, IL-4 and IL-17 were searched from Pubmed Nucleotide Search (http://www.ncbi.nlm.nih.gov/pubmed/). The Genbank accession numbers for each cytokine were NM_000619.2, M13982.1 and NM_002190.2, respectively.

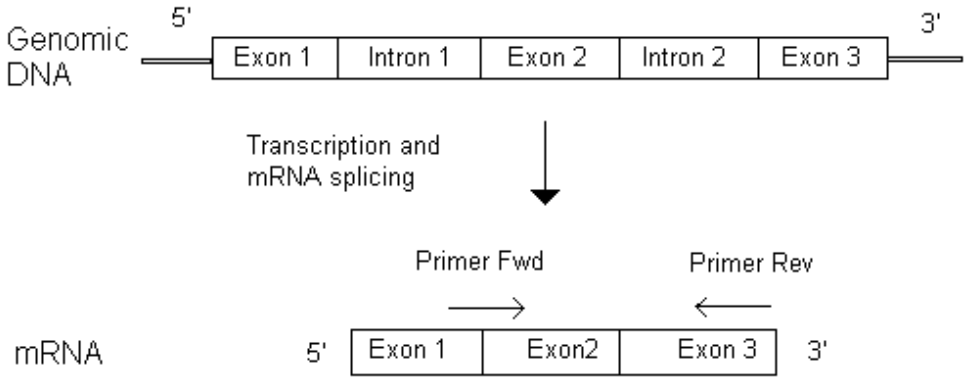

Figure 7. Locations of the forward and reverse primers after transcription and mRNA splicing. Modified from Applied Biosystems Training course Basic PCR 2006.

The primers were blasted in ncbi BLAST (http://www.ncbi.nlm.nih.gov/blast/Blast.cgi) that compares nucleotide sequences and determines sequence homology ensuring that the primers were specific for the target cytokine mRNA. In addition, primer sequences were processed with OligoCalc: Oligonucleotide Properties Calculator (http://www.basic.northwestern.edu/biotools/oligocalc.html) that reveals self-complementarity, hairpin formation and primer-dimer formation of the primer sequences.

4.6.2. Reaction mixtures and optimization of the primer concentrations

The real-time PCR kit applied was Finnzymes DyNAmo™ Flash SYBR® Green qPCR Kit. The performance of the kit is based on a SYBR Green I fluorescent dye and a hot start version of a modified *Thermus brockianus* DNA polymerase alias modified Tbr polymerase, in which a DNA-binding domain attached to the polymerase improves the stability of the polymerase-DNA complex. The kit includes Master mix and 50xROX passive reference dye. The master mix contains Tbr DNA polymerase, SYBR Green I, optimized PCR buffer, 5mM $MgCl_2$ and dNTP mix. The passive reference dye does not participate in the real-time PCR reaction and its fluorescence stays constant during the real-time PCR reaction. The passive reference dye is used to normalize the non-PCR related fluorescence signal variation. Typically, good results are obtained with primer concentration 0.5µM for both forward and reverse primers, but the optimal primer concentration varies between 0.3µM and 1µM. The total reaction mixture volume is 50µl and the primer and water volumes can be altered in the optimization process (Table 4). More information is available in Finnzymes DyNAmo™ Flash SYBR® Green qPCR Kit Instruction manual.

Table 4. One portion of the standard real-time PCR mixture.

Reaction mixture (1x)	**Volume (µl)**
Master mix	25
10µM Primer Forward	X
10µM Primer Reverse	X
ROX Passive refence dye	1
dH_2O	add to 50µl
cDNA sample	5
Total	50

IFN-γ, IL-4 and IL-17 reaction mixtures were tested with 0.2-0.6 M primer concentrations with 0.05µM intervals and the most optimal concentration for each cytokine was chosen. The optimal primer concentrations were 0.4µM for IFN-γ, 0.3µM for IL-4, 0.45µM for IL-17 and 0.3µM for TBP. The selection of the optimal primer concentrations is presented in Chapter 5.1.1. The optimal reaction mixtures are represented below, from which TBP reaction mixture was optimized before in the Virology Laboratory (Table 5).

Table 5. Optimal real-time PCR reaction mixtures for each gene.

Reaction mixture 1x	**TBP 0.3µM Volume (µl)**	**IFN-γ 0.4µM Volume (µl)**	**IL-4 0.3µM Volume (µl)**	**IL-17 0.45µM Volume (µl)**
Master mix	25	25	25	25
10µM Primer Forward	1.5	2	1.5	2.25
10µM Primer Reverse	1.5	2	1.5	2.25
ROX passive refence dye	1	1	1	1
dH_2O	16	15	16	14.5
cDNA sample	5	5	5	5

4.6.3. Optimization of the real-time PCR cycle

The T_m values of the primers were represented in Table 3 and they varied from +54ºC to +59.4ºC. The recommended annealing temperature is +60ºC, but different annealing temperatures +56ºC, +58ºC and +60ºC were tested for all cytokines. Annealing temperature +60ºC was selected, since the other tested temperatures did not improve the performance of the real-time PCR method for the cytokines. The results of the cycle optimization are represented in Chapter 5.1.2. The real-time PCR

was carried out using Applied Biosystems HT7900 instrument and the real-time PCR program is shown below.

Real-time PCR program:

1. First denaturation at +95ºC for 7 minutes.
2. Denaturation at +95ºC for 10 seconds.
3. Annealing/extension at +60ºC for 30 seconds.
4. Data collection at +78ºC for 30 seconds.
5. 40 repeats of steps 2-4.
6. Final extension +60ºC for 1 minute.
7. Melting curve from +60ºC to +95ºC.
8. Infinite hold at +4 ºC.

4.6.4. Specificity and sensitivity

Specificity of the real-time PCR was tested for each three cytokines using mononuclear cell samples from four healthy volunteers. After the real-time PCR run the amplified cDNA was identified in agarose gel electrophoresis. Sample dilution series (10^{0}-10^{-7} and 2^{0}-2^{-6}) were used to define the sensitivity of the method. Power series of ten were done so, that the first $10^{\wedge 0}$ dilution contained 45µl dH_2O and 5µl cDNA from RT-reaction, which was then further diluted with a ratio of 1:10. In power of two series the dilution ratio was 1:2. The results are shown in Chapter 5.1.3.

4.6.5. Real-time PCR protocol

The real-time PCR was carried out according to the guidelines of Applied Biosystems. A scheme of sample locations on a 96-optical well plate was planned on a worksheet and the master mixture volumes were calculated according to Table 5 before starting the process. First, the master mixture was prepared and then 45µl master mixture and 5µl cDNA from RT-reaction were loaded per well on the 96-optical well plate. The plate was covered with an optical adhesive cover and centrifuged at 1120rpm at +4ºC for 1 minute. A compression pad was sealed on the top of the reaction plate and the plate was placed into Applied Biosystems HT7900. The run was started using program

described in Chapter 4.6.3. with SDS Enterprise Database by Applied Biosystems. After the run the plate was stored for gel electrophoresis at +4ºC.

4.7. Agarose gel electrophoresis

The cDNA samples were identified with agarose gel electrophoresis after the real-time PCR amplification. Agarose gel electrophoresis is a simple method for separating, identifying and purifying DNA fragments. Nucleic acids are negatively charged and they move towards positive electrode in an electric field. In a porous agarose gel DNA fragments are separated according to their size, so that smaller fragments move faster and further than larger fragments. The DNA bands on agarose gel are stained by the dye ethidium bromide, which emits fluorescence under ultraviolet light, when it is bound to DNA. (Alberts B et al., 2002) The size of the DNA fragments can be determined by comparing them to the DNA size standard.

The agarose gel electrophoresis was performed according to the standard protocol of the Department of Virology at the University of Tampere. Agarose gel was prepared as shown in Table 6.

Table 6. Contents of the 2 % agarose gel.

2% Gel
200ml ddH_2O
4g Agarose (Promega, Cat. V3125)
4ml 50xTAE buffer
2 drops of Ethidium bromide (Amresco, Cat. E406)

First, agarose was weighed with Mettler PJ 400 scale. ddH_2O, Agarose and 50xTAE buffer were mixed and boiled in a microwave oven until all the agarose was dissolved. Then, ethidium bromide was added to the mixture and the mixture was cooled for 10-15 minutes. Two combs were put into the 15x20cm gel tray and the mixture was poured in. Air bobbles were removed and the liquid mixture was cooled for 30 minutes. The combs were removed from the solid gel and the gel was transferred to a gel electrophoresis tank filled up with 1xTAE buffer.

Each sample was prepared by adding 2µl of 6x loading buffer to 10µl of real-time PCR product. The samples were loaded to the wells and 3µl of a 100bp DNA size standard (MBI Fermentas, Cat. SM0242) was added into one well in each run. The run was executed at 100V for 90 minutes.

Finally, the gel was visualized under UV light and photographed with AlphaDigiDocTM. The expected amplicon sizes of the PCR product were 202bp for IFN-γ, 217bp for IL-4, 245bp for IL-17 and 227bp for TBP (Table 3).

4.8. *In vitro* white blood cell cultures

The blood samples were taken from healthy volunteers into 10ml CPT-tube. Mononuclear cells were purified by centrifugation at 2770rpm for 20 minutes at room temperature. The plasma and mononuclear cells were mixed and placed into a 10ml Sarstedt tube, which was then centrifuged at 1700rpm for 15 minutes at room temperature. After centrifugation mononuclear cells formed a solid pellet, which was removed into a 50ml tube and washed once with 40ml of RPMI by centrifugation at 2000rpm for 10 minutes at room temperature. RPMI was removed with suction and the cells were diluted in 1ml of medium and calculated under the microscope (10µl cell suspension and 90µl Typan blue dye). Finally, in 96-well sterile round-bottom microtitre plate, the cell concentration was adjusted to 200 000 cells in 100µl of the cell culture medium per well. The medium components are shown in Table 7.

Table 7. Cell culturing medium.

Medium components	**Volume (ml)**
RPMI (GIBCO 31870)	3.52
Inactivated human AB-serum (Cambrex Cat. 14-498E)	0.40
PEN- STREP (PAA Cat.P11-010 100mM)	0.04
L-glutamin (GIBCO 25030 200mM)	0.04
Total	4

The cells were stimulated with a mixture of soluble anti-CD3 (10µg/ml) and soluble anti-CD28 (1µg/ml) (R&D systems Cat.MAB100 and Cat.MAB342) as well as with infective enteroviruses representing serotypes CBV1, CBV4, CAV9, Echo 9, Echo 11 and Echo 30 (ATCC prototype strains) and medium control. The titer of viruses per well was 5PFU, which equals about million viruses per well. The cells were harvested after 48 hours incubation at +37°C and 4 concurrent wells were combined into one tube. The tube was centrifuged at 1500rpm for 10 minutes at room temperature and the cell pellet was pipettted into Giagen RLT buffer containing β-mercaptoethanol. These samples were then stored at -70°C until used for RNA isolation and real-time PCR.

5. RESULTS

The results are shown in three sections including real-time PCR optimization, RNA isolation from buffy-coat samples and *in vitro* stimulations of white blood cell. As a reminder for the following considerations, the lower the CT value, the higher the amount of RNA present in the original sample.

5.1. Real-time PCR optimization for the analyses of mononuclear cell samples

The results of the real-time PCR optimization are presented here to demonstrate the selection of primer concentration, optimization of real-time PCR cycle conditions, confirming specificity and sensitivity of the real-time PCR and analyses of clinical samples (Figure 8). The samples were mononuclear cell samples obtained from healthy volunteers.

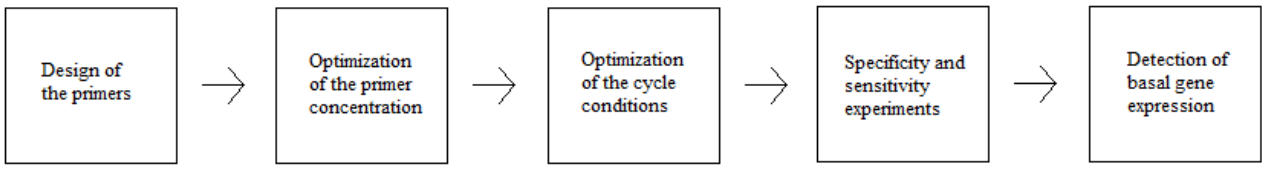

Figure 8. Stages of the real-time PCR optimization process.

5.1.1. Selection of primers and primer concentrations

Primers for each three cytokines were designed as described in Chapter 4.6.1. For IFN-γ six different primer pairs, for IL-4 five primer pairs and for IL-17 eight primer pairs were tested to find out, which primer pairs perform best in real-time PCR giving the lowest CT values, optimal dissociation curves and clear bands in agarose gel electrophoresis. Three best-performing primer pairs for each cytokine were selected for further optimization to test different primer concentrations ranging from 0.2µM to 0.6µM. One primer pair with optimal primer concentration was selected for each cytokine to be used in the final real-time PCR method. The final primer sequences are shown in Table 3 and the optimal real-time PCR reaction mixtures in Table 5.

5.1.2. Optimization of the real-time PCR cycle conditions

Three annealing temperatures +56ºC, +58ºC and +60ºC were tested for each of the three cytokines and TBP to optimize the real-time PCR cycle. Mononuclear cell samples were obtained from a healthy volunteer. The CT values of these experiments are shown in Table 8. Annealing temperature +56ºC gave the weakest results and there was no significant difference between annealing temperatures +58ºC and +60ºC, so the standard annealing temperature +60ºC was selected as described in Chapter 4.6.3.

Table 8. CT values for each gene at annealing temperatures +56ºC, +58ºC and +60ºC. Average CT values of three concurrent real-time PCR runs are shown.

Gene	Annealing temperature +60°C	Annealing temperature +58°C	Annealing temperature +56°C
TBP	24.4	24.8	26.1
IFN-γ	31.0	32.6	33.9
IL-4	31.6	31.6	33.0
IL-17	39.2	39.2	Undetermined

5.1.3. Specificity and sensitivity of amplification

One mononuclear cell sample of a healthy volunteer was treated with DNase and another sample was not treated with DNase during the RNA isolation as described in Chapter 4.4.1. to study a possible interfering effect of the genomic DNA. Cytokines and TBP were tested for both samples. Any non-specific bands were not detected on the gel neither in DNAse treated nor non-treated sample indicating, that the primers were specific for the target gene and no genomic DNA was amplified (Figure 9).

Dilution series of 2^{-n} were made from mononuclear cell samples and analyzed for the expression of each of the genes (Table 9). PCR products of all these samples were also run in the agarose gel electrophoresis showing that the bands were sharp and specific (data not shown). Such dilution series were also done for white blood cells, which were stimulated with enteroviruses *in vitro* to define the slope of dilution series and real-time PCR efficiency for further analysis with Pfaffl equation.

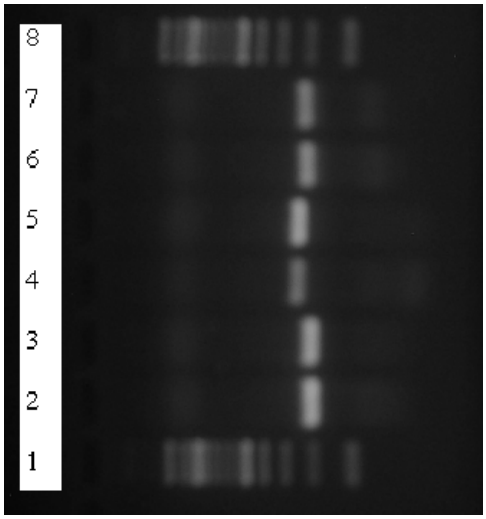

Figure 9. Effect of DNase treatment during RNA isolation step on the accuracy of the real-time PCR. DNase treated and non-treated samples are shown on the gel as following: Line 1 is molecular marker, line 2 is DNase-treated IFN-γ, line 3 is non-DNase treated IFN-γ, line 4 is DNase-treated IL-4, line 5 is non-DNase-treated IL-4, line 6 is DNase-treated IL-17, line 7 is non-DNase-treated IL-17 and line 8 is molecular marker.

Table 9. CT values of 2^{-n} dilution series. Average CT values of three concurrent experiments are presented for each gene.

Dilution	TBP	IFN-γ	IL-4	IL-17
2^{0}	23.9	22.3	31.0	25.4
2^{-1}	25.1	23.1	32.6	26.6
2^{-2}	26.2	24.3	33.9	28.0
2^{-3}	27.1	25.7	34.8	28.7
2^{-4}	28.1	26.1	35.8	29.6
2^{-5}	29.0	27.3	37.7	31.1

5.1.4. Detection of basal gene expression

The ability of the real-time PCR methods to detect basal gene expression of the three cytokines and TBP was tested by analyzing non-stimulated mononuclear white blood cells of four healthy volunteers. CT values indicate that the method works well for all samples taken from these individuals (Table 10). Basal gene expression level was detected in all except one of the samples suggesting that the method is sensitive enough to detect even low basal gene-expression rates. In the gel electrophoresis all the bands were sharp and of the right molecular size, but there were differences in the sharpness and brightness of the bands (data not shown).

Table 10. CT values of the proinflammatory cytokines and TBP. Mononuclear cell samples were obtained from four healthy volunteers (Subjects 1-4). CT values represent an average of two experiments.

Gene	Subject 1	Subject 2	Subject 3	Subject 4
TBP	24.4	24.6	23.5	26.6
IFN-γ	31.0	31.4	30.1	31.0
IL-4	31.6	32.5	30.1	35.0
IL-17	39.2	39.0	39.3	Undetermined

5.2. RNA isolation from buffy-coat samples

This chapter summarizes the results considering the optimization of RNA isolation from frozen buffy-coat samples for the real-time PCR analyses. Different kits and protocols were tested for this purpose. Previous experiments at the Department of Virology revealed that RNA isolation with Qiagen RNeasy® Mini Kit with Animal Cells Spin protocol and homogenization with QIASchredder columns, did not work properly for frozen buffy-coat samples, even though it worked well for frozen mononuclear cell samples. Therefore, there was a need for a proper method. The frozen buffy-coat samples were obtained from healthy volunteers and from the children participating in the DIPP study. The CT values represented absolute amounts of RNA and efficacy of RNA isolation was evaluated by comparing these CT values. The differences of the samples are explained in Chapter 4.3.2.

5.2.1. RNA isolation with Qiagen RNeasy® Mini Kit modified protocols

RNA isolation from frozen buffy-coat samples with Qiagen RNeasy® Mini Kit was tested using Modifications 1-4 (see Chapter 4.4.2. and Table 1). The buffy-coat samples were obtained from healthy volunteers and from the children participating in the DIPP study. The CT values obtained using Modifications 1 and 2 (sample volume 200-100 µl) are presented in Table 11. Similarly, the CT values obtained using Modifications 3 and 4 (sample volume 100-200µl) are demonstrated in Table 12.

Table 11. CT values received using Qiagen RNeasy® Mini Kit with Modifications 1 and 2 for buffy-coat samples having a 200-1000µl final volume. CT values are represented as an average of two or three concurrent.

RNA isolation method: Modification 1				
Subject	**TBP**	**IFN-γ**	**IL-4**	**IL-17**
Healthy volunteer 1	28.8	34.2	35.0	32.3
DIPP study participant 1	29.9	32.7	37.1	34.6
DIPP study participant 2	31.9	36.2	38.4	32.3
RNA isolation method: Modification 2				
Subject	**TBP**	**IFN-γ**	**IL-4**	**IL-17**
Healthy volunteer 1	29.7	33.4	34.0	34.7
DIPP study participant 3	27.6	29.9	35.9	39.5
DIPP study participant 4	28.0	30.0	36.1	36.9

Table 12. CT values received using Qiagen RNeasy® Mini Kit with Modifications 3 and 4 for buffy-coat samples having a 100-200µl final volume. CT values are represented as an average of two or three concurrent.

RNA isolation method: Modification 3				
Subject	**TBP**	**IFN-γ**	**IL-4**	**IL-17**
Healthy volunteer 1	32.1	35.3	36.7	36.7
DIPP study participant 5	28.3	31.8	36.2	35.2
DIPP study participant 6	32.1	36.1	39.8	39.1
RNA isolation method: Modification 4				
Subject	**TBP**	**IFN-γ**	**IL-4**	**IL-17**
Healthy volunteer 1	31.1	34.8	34.4	32.0
DIPP study participant 7	29.5	34.0	36.2	35.8
DIPP study participant 8	27.9	31.7	35.9	35.7

In these analyses both CT values and results from gel electrophoresis were taken into consideration. Modifications 2 and 4 gave slightly better CT values than Modifications 1 and 3. In gel electrophoresis specific bands were invariably detected for TBP, IFN-γ and IL-17, while IL-4 showed more variation. This variation in IL-4 specific amplification included primer-dimer formation recognized as small molecular size bands on the gel as well as a lack of PCR product. This may be related to relatively low basal expression of IL-4 in the buffy-coat samples.

5.2.1.1. Effect of β-mercaptoethanol in RLT lysis buffer on RNA isolation

In Qiagen RNeasy® Mini Kit with Animal Cells Spin protocol (see Chapter 4.4.1) the addition of β-ME (β-mercaptoethanol) into RLT lysis buffer is an optional procedure, which is recommended if the sample contains a significant amount of nucleases. The effect of β-ME was tested for both mononuclear cell samples and buffy-coat samples having the final volume of 100-200µl. The test samples were received from healthy volunteers. CT values from this experiment are shown in Table 13.

Table 13. The effect of β-ME on the CT values of buffy-coat and mononuclear cell samples. CT values were calculated as an average of three concurrent. β-ME was added on A samples, but not on B samples.

Sample	β-ME	TBP	IFN-γ	IL-4	IL-17
Buffy-coat A	yes	28.3	30.2	35.1	36.3
Buffy-coat B	no	26.7	29.2	34.0	32.7
Mononuclear cells A	yes	24.4	26.3	31.6	36.9
Mononuclear cells B	no	24.6	27.0	31.8	37.7

The gel electrophoresis results confirmed specific amplification, except for IL-4 which did not provide visible band for buffy-coat A. β-mercaptoethanol in RLT lysis buffer enhanced the RNA isolation from mononuclear cell samples, but reduced the RNA isolation from buffy-coat samples.

5.2.2. Experiments with Qiagen Oligotex® Direct mRNA Mini Kit

The mRNA isolation from frozen buffy-coat samples having a final volume 100-200µl was tested with Qiagen Oligotex® Direct mRNA Mini Kit with Animal Cells protocol. The Oligotex® kit protocol is available in Qiagen Oligotex® Handbook Second Edition (May 2002). The buffy-coat samples were received from volunteer and the CT values are represented in Table 14.

Table 14. CT values of the mRNA isolation with Qiagen Oligotex® Direct mRNA Mini Kit. Sample I was homogenized with 20G needle and syringe and sample II was homogenized with QIAShredders. CT values are calculated as an average of three concurrent.

Sample	TBP	IFN-γ
Buffy-coat I	33.1	36.2
Buffy-coat II	34.1	35.3

Two different methods were used for the homogenization of the sample (Buffy-coat I and Buffy-coat II, respectively). CT values were weak, which means that the RNA isolation was not effective.

5.2.3. Experiments with Qiagen AllPrep® DNA/RNA/Protein Mini Kit

The mRNA isolation from frozen buffy-coat samples named as Buffy-coat III-VI having a final volume of 100-200µl was also tested using Qiagen AllPrep® DNA/RNA/Protein Mini Kit with Cells protocol. The advantage of this kit is, that not only RNA, but also DNA and proteins are isolated. Moreover, the RNA isolation procedure is almost similar to RNeasy® Mini Kit protocol described in Chapter 4.4.1. The protocol is available in Qiagen AllPrep® DNA/RNA/Protein Mini Handbook (December 2007). The buffy-coat samples were obtained from a volunteer and the CT values are represented in Table 15

Table 15. CT values of the Qiagen AllPrep® DNA/RNA/Protein Mini Kit experiments. Buffy-coat samples III and IV were both homogenized with 20G needle and syringe, while samples V and VI were homogenized with QIAShredders. Sample III and V are DNase treated in RNA purification step and samples IV and VI are not DNase treated in that step. CT values are calculated as an average of three concurrent.

Sample	Homogenization	DNase	TBP	IFN-γ	IL-4	IL-17
Buffy-coat III	20G needle + syringe	Yes	28.0	33.5	34.4	37.4
Buffy-coat IV	20G needle + syringe	No	28.6	34.9	33.5	28.4
Buffy-coat V	QIAShredders	Yes	33.7	37.3	35.6	Undetermined
Buffy-coat VI	QIAShredders	No	33.1	Undetermined	36.7	Undetermined

The CT values indicated quite successful RNA isolation especially when the homogenization was done with 20G needle and syringe.

5.3. Results of the *in vitro* white blood cell stimulations

Mononuclear cells obtained from two volunteers were stimulated by different enterovirus serotypes as described in Chapter 4.8. The mathematical analyses of relative gene expression were done with Pfaffl equation (See Chapter 2.3.4.). The dilution coefficient was 2, so the efficiency was calculated as $E = 2^{[-1/slope]}$. AntiCD3/antiCD28 stimulated cells were used to calculate the standard line, slope and correlation coefficient needed in this formula. Standard line represents the efficiency of the real-time PCR and eliminates the effect of inter-PCR-variations on test results. The relative

expression ratios of white blood cell stimulation are shown numerically in Table 16. Considering relative expression ratios, the larger ratio refers to high expression. In this experiment all the calculations were made from average CT values obtained from 3 concurrent experiments. Each sample was also processed with gel electrophoresis and sharp bands of right size were observed for all tested cytokines.

Table 16. Relative gene expression ratios of the proinflammatory cytokines after *in vitro* stimulation of mononuclear cells with different enterovirus serotypes. CT values are calculated as an average of three concurrent. (CBV1 = Coxsackievirus B1, CBV4 = Coxsackievirus B4, CAV9 = Coxsackievirus A9, Echo9 = Echovirus type 9, Echo11 = Echovirus type 11, Echo 30 = Echovirus type 30)

Donor 1			
Stimulant	**IFN-γ**	**IL-4**	**IL-17**
medium control	1.0	1.0	1.0
CBV1	52.3	1.6	1.3
CBV4	48.2	1.8	2.0
CAV9	70.1	1.4	1.6
Echo9	3.4	1.4	0.6
Echo11	169.1	2.2	2.4
Echo30	165.7	1.3	4.2
CD3/CD28	135.3	0.6	1541.5
Donor 2			
Stimulant	**IFN-γ**	**IL-4**	**IL-17**
medium control	1.0	1.0	1.0
CBV1	17.8	0.8	1.7
CBV4	3.7	1.4	0.9
CAV9	9.5	1.2	2.4
Echo9	7.6	1.3	1.0
Echo11	176.2	0.7	1.0
Echo30	16.9	0.8	2.2
CD3/CD28	32.7	0.9	677.5

The relative gene expression ratios from Table 16 are represented graphically below in Figures 10-12. The results show that enteroviruses induce clear IFN-γ responses while they did not induce IL-4 expression. IL-17 responses were moderately induced.

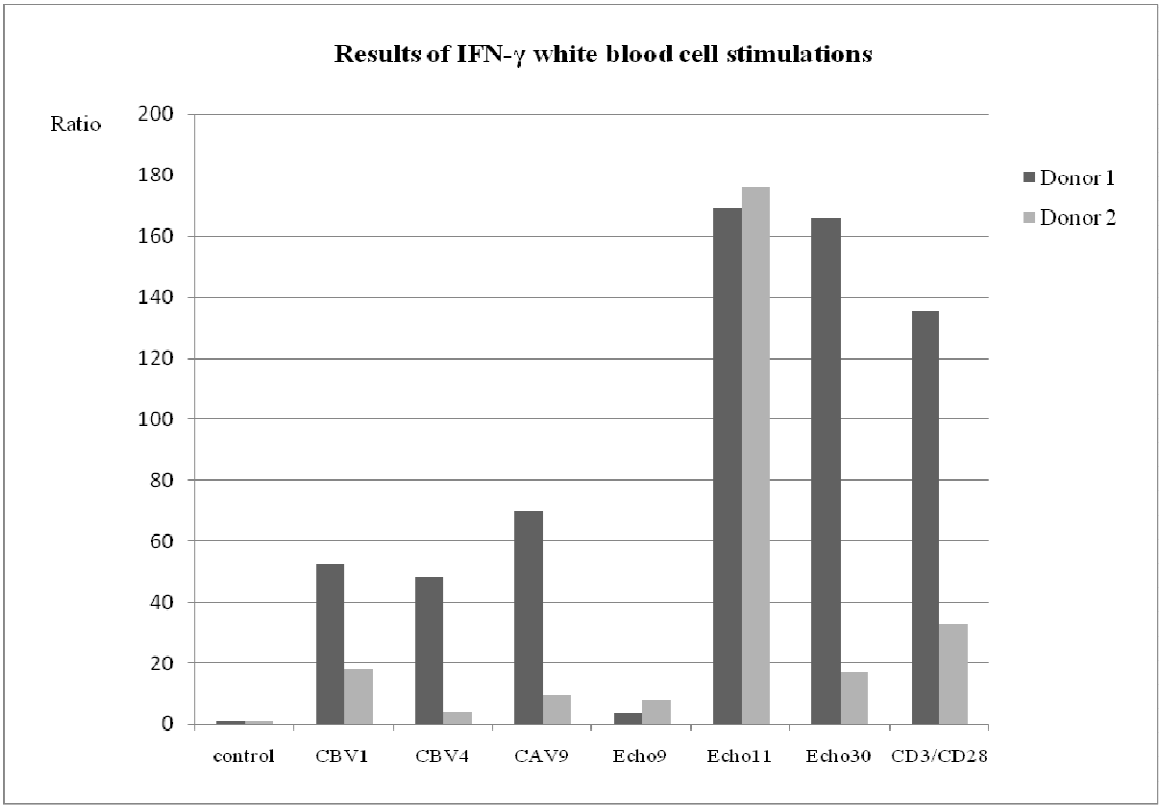

Figure 10. Relative gene expression ratios for IFN-γ in mononuclear cell cultures stimulated with different enterovirus serotypes.

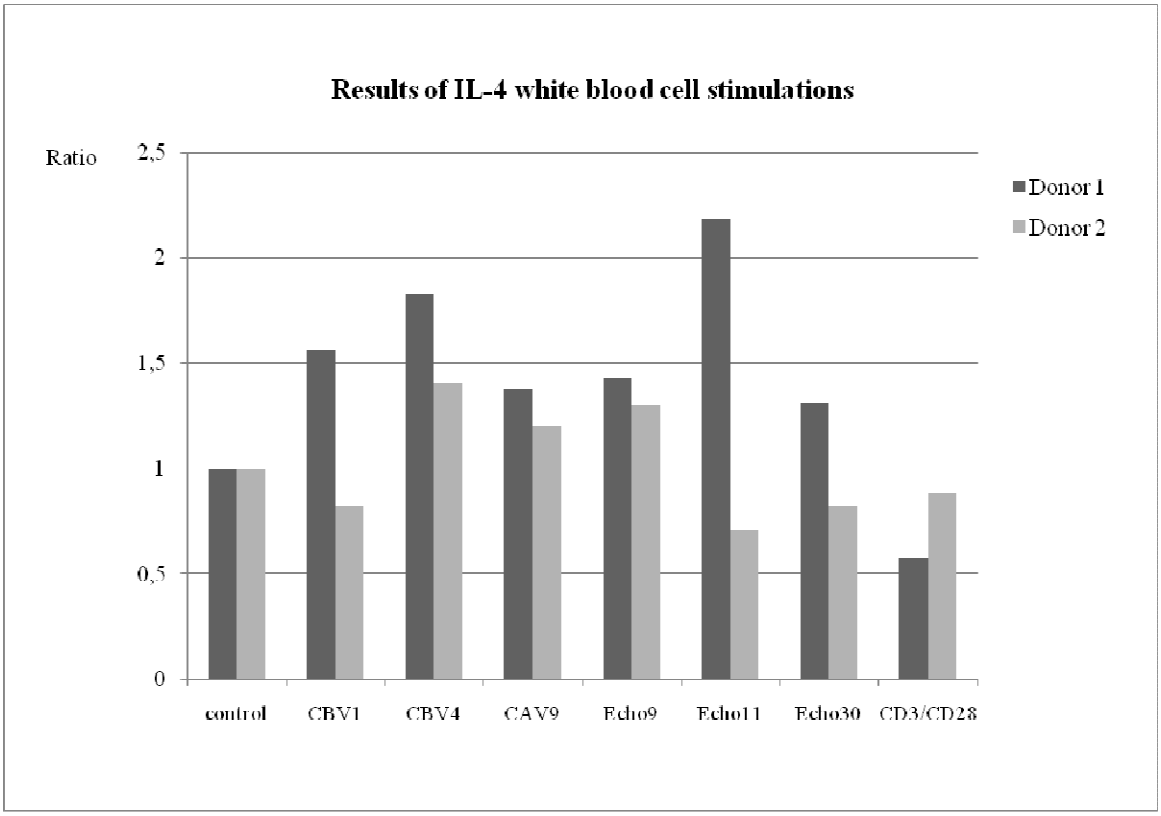

Figure 11. Relative gene expression ratios for IL-4 in mononuclear cell cultures stimulated with different enterovirus serotypes.

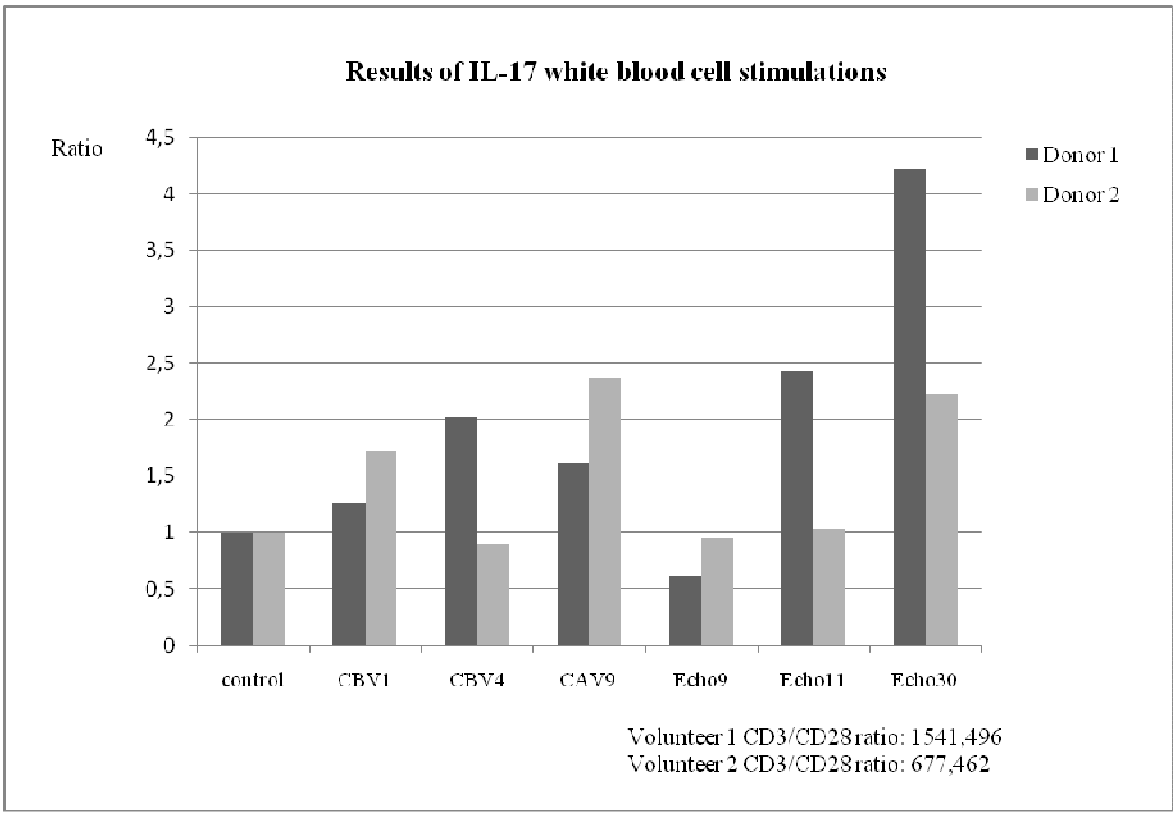

Figure 12. Relative expression ratios for IL-17 in mononuclear cell cultures stimulated with different enterovirus serotypes.

6. DISCUSSION

The main aim of the present study was to develop real-time PCR methods for reliable detection of the expression of proinflammatory cytokines in white blood cells, which have been stored at -70°C or -136°C for several years. The study included development of real-time PCR assay for three cytokines (IFN-γ, IL-4 and IL-17) for two sample types including both mononuclear cells and buffy-coat.

6.1. Optimization of the real-time PCR assay

The real-time PCR was optimized by choosing the optimal primer concentrations and cycle conditions as described in Chapters 5.1.1. and 5.1.2. The specificity and sensitivity of PCR amplification were confirmed by detection of single band of right molecular weight in agarose gel electrophoresis and by dilution series for each of the three cytokines IFN-γ, IL-4 and IL-17. It was confirmed that the methods were not sensitive for possible genomic DNA contamination, since DNAse-treatment of isolated RNA had no effect on the results. However, the DNAse treatment was done for all samples to ensure the quality of the assay.

Basal cytokine expression levels were low in peripheral blood cells and were not always detected by even this kind of sensitive assay when high sample dilutions were tested (10^{-n} dilution series). However, cytokine expression was detected in undiluted samples and in lower sample dilutions such as the 2^{-n} dilution series as shown in Table 9. The CT values decreased with increasing dilution coefficient suggesting that the real-time PCR method was working correctly. The expression of cytokines was also tested in different individuals to evaluate the ability of the assay to detect individual variation in gene expression. There was variation between individuals in the house-keeping gene expression, in the cytokine expression and also in the relative gene expression ratios. Therefore, it is important to normalize the samples with Pfaffl equation to find out true differences in target gene expression between individuals.

The expression of proinflammatory cytokines arise temporary in inflammation. Their expression can also be induced *in vitro* in cultured white blood cells by different stimuli such as viruses or polyclonal activators of the immune system (e.g. anti-CD3 and anti-CD28 antibodies). Therefore,

the induction of the proinflammatory cytokines was tested in mononuclear cell cultures, which were stimulated by different enterovirus serotypes and anti-CD3 and anti-CD28 antibodies as a control. These experiments confirmed that the real-time PCR methods were able to detect clear increases in the cytokine expression levels during *in vitro* stimulation (see Chapter 5.3. and 6.3.).

The real-time PCR method worked well for both fresh and frozen mononuclear cell samples, but there were some difficulties in the analysis of buffy-coat samples. The average CT values were higher in buffy-coat samples than in mononuclear cell samples indicating lower gene expression and in some cases IL-4 was not amplified at all. The reason may be that the buffy-coat samples are contaminated with eryhrocytes and are not as pure as mononuclear cell samples. On the other hand, the basal IL-4 expression levels may indeed be negligible in unstimulated samples. Low IL-4 expression levels may lead to primer-dimer formation, because primer-dimer formation and PCR product amplification are competing processes. In a way this phenomenon is in line with the literature. The IL-4 expression is noticed to be low in healthy controls and the secretion of IL-4 is increased in individuals having allergic disorders meaning that the T_H2 regulation is not related to enteroviral stimuli (Coëffier et al., 2005). In addition, Kvarnström et al. suggest that especially the expression of IL-4 is decreased during freezing the cells, and point out the importance of investigation of the effects of freezing before using frozen cells in studies of *in vitro* cytokine secretion (Kvarnström et al.,2004).

The SYBR Green dye binds to DNA minor groove in a non-sequence-specific manner. Thus, the same amount of DNA gives rise to the same fluorescence signal level despite the amplified sequence. Therefore, it is important to have approximately equal template lengths for all the amplified sequences as represented in Table 3. Otherwise the results may be biased by varying length of the PCR product.

In this study the real-time PCR method was optimized successfully for the three cytokines. The results suggest that the method can be used reliably for the detection of cytokine expression in human white blood cells. It proved also to be applicable for different sample types such as mononuclear cells and buffy-coat samples, and it even worked for frozen samples. This real-time PCR method can be used to analyze cytokine expression levels in clinical samples (fresh and frozen white blood cells) and in cell cultures allowing a wide range of applications. The Department of Virology will use this method to study cytokine responses which are induced in enterovirus

infections and in immune-mediated diseases. One possible drawback of these assays is related to the challenge caused by the impurities of frozen buffy-coat samples. However, the results suggest that these problems can be avoided by selection of the most optimal RNA isolation method.

6.2. Optimization of RNA isolation method for buffy-coat samples

RNA isolation from buffy-coat samples, especially if frozen, is challenging and successful RNA isolation protocols have not previously been published for frozen buffy-coat samples. However, that kind of samples have been collected in many clinical studies and there is a clear demand for this kind of protocol. The Department of Virology at the University of Tampere has stored a large amount of buffy-coat at -70°C and at -136°C during the past 10 years in the DIPP study. Therefore, RNA isolation from frozen buffy-coat samples was set as one important goal of this study. Different RNA isolation methods were tested including Qiagen RNeasy® Mini Kit with modified protocols as well as Qiagen Oligotex® Direct mRNA Mini Kit with Animal Cells protocol and Qiagen AllPrep® DNA/RNA/Protein Mini Kit with Cells protocol.

The Oligotex® kit is expensive and the cost of one processed sample is approximately 50 Euros. The advantage of this kit is that only messenger RNA is isolated based on the biochemical properties of poly-A tail. In spite of the advanced new technology of this kit, the CT values obtained with the real-time PCR turned out to be weak as demonstrated in Table 14. The high cost was also the reason why this method was tested only for two genes, TBP and IFN-γ. Based on these argumentations, this kit was not selected for further optimization for frozen buffy-coat samples.

The unquestionable advantage of the AllPrep® is that not only RNA, but also DNA and proteins are isolated. So, the unique DIPP samples would be utilized more efficiently than if only RNA is isolated. Moreover, the CT values indicated quite high concentration of isolated RNA, especially when the homogenization was done with 20G needle and syringe as shown in Table 15. However, the laboratory procedure was complicated. Due to the varying volumes of buffy-coat samples, the use of this kit would be very labor-intensive and time-consuming way to isolate RNA. In the DIPP study the sample volume was standardized to be 100-200µl for samples taken after the year 2001 and for those samples this kit could be feasible. In other words, AllPrep® could be used for DIPP samples taken after the year 2001 while it may be not be optimal for samples taken before that time because of the varying sample volume 200-1000µl.

Modified protocols of Qiagen RNeasy® Mini Kit worked well for all kind of buffy-coat samples, and would be optimal for RNA isolation in the DIPP study. Based on the CT values obtained in real-time PCR (Tables 11 and 12) the best Qiagen RNeasy® Mini Kit RNA isolation method is Modification 2 for buffy-coat samples with 200-1000µl final sample volume and Modification 4 for buffy-coat samples with 100-200µl final sample volume (see Chapter 4.4.2. to get more information about the Modifications). In Modification 2 the homogenization is done using 20G needle and syringe and one volume of 96-100% ethanol is added to homogenates to avoid dilution of the sample. In Modification 4, 900µl of RLT cell lysis buffer is used instead of the original volume 600µl and the homogenization is done with 20G needle and syringe. One volume of 70% ethanol is added to the lysate (approximately 1100µl). Thus, the protocols of Modifications 2 and 4 are approximately equal and they could be used simultaneously for RNA isolation of different buffy-coat sample types despite the variations between these samples.

The features of different kits and protocols are compared and summarized in Table 17. Features are scored with scaling 0-5 and the total scores of the kits are represented. This table is in line with the previous discussion, since RNeasy® Mini Kit Modifications 2 and 4 got the highest total score.

Table 17. Different features of the tested kits are compared in the table. Each feature has a score of 0-5, where score 5 represents the best performance. The scores of the features are summed and presented in a total score column ranging 0-15. Questionmark (?) symbolizes the fact, that the amount and quality of DNA and protein purified with AllPrep® were not tested. Therefore, this feature cannot be scored reliably.

Qiagen RNA isolation Kit	RNA isolation	Protocol simplicity	Price	DNA and protein isolation	Total score
Oligotex®	0	5	0	0	5
AllPrep®	4	0	4	5(?)	8-13
RNeasy® Modifications 1 and 3	4	5	5	0	14
RNeasy® Modifications 2 and 4	5	5	5	0	15

In addition, the effect of β-ME in RLT lysis buffer in Qiagen RNeasy® Mini Kit was tested and the results were shown in Table 13. The presence of β-ME in RLT lysis buffer enhanced the RNA isolation from mononuclear cell samples, but the effect was opposite in buffy-coat samples. Therefore, the β-ME in RLT lysis buffer should not be used when handling buffy-coat samples. The CT values were very good with these buffy-coat samples which were stored frozen for only a few

days. Therefore, the results are not necessarily comparable to buffy-coat samples, which have been stored frozen for prolonged periods. However, the importance of the β-ME in RNA isolation from mononuclear cell samples was clearly demonstrated.

Successful RNA isolation from frozen buffy-coat samples is important for efficient use of the biobank of the DIPP study. Moreover, the ongoing process of collecting buffy-coat samples has certain advantages in cost benefits compared to more complex purification of mononuclear cells. This study shows that Qiagen RNeasy® Mini Kit with modified protocols can be used for the RNA isolation from frozen buffy-coat samples and that these samples can be used reliably for the analyses of cytokine expression by real-time PCR.

6.3. *In vitro* stimulations of white blood cells

The results indicate that some enterovirus serotypes clearly induced the expression of IFN-γ and IL-17 while they did not induce the expression of IL-4. This is in line with the fact that these viruses have been connected to type 1 diabetes where T_H1 and T_H17 cells play an important role in the pathogenesis. Especially serotypes CBV4, CAV9, Echo11 and Echo30 caused an increase in cytokine expression. There was up to a 170-fold increase in IFN-γ expression with some enterovirus serotypes, while the greatest ratios for IL-17 were four-fold. Naturally, variation between individuals exists, which can also be observed from results represented in Chapter 5.3. The cells were obtained from volunteers at the age of 25-30 years and the individual differences may arise from genetic factors and from the infection history of the individual. IL-4 expression levels of *in vitro* white blood cell stimulations were opposite and enterovirus serotypes were not found to stimulate IL-4 expression, that may suggest different regulation of IL-4 compared to the other tested cytokines. Its expression may be easier to find in other kind of conditions such as in anti-allergen specific responses in IgE-sensitized individuals. In some cases IL-4 expression even decreased during enterovirus stimulation.

This reflects previous literature showing that the increased function of T_H1 and T_H17 cells is connected to autoimmune diseases (Dong, 2008 and Kurts, 2008), and it is supposed that enteroviruses can stimulate these T cell responses (Viskari et al., 2004). In addition, Li and Dufour suggest that IFN-γ could be used as a biomarker to detect viral response. T cells showed specific IFN-γ response for coxsackievirus B3 (CVB3) or coxsackievirus B4 (CVB4). (Li & Dufour, 2008)

Literature also shows that T_H2 cells are regulated with different mechanisms independently of enterovirus stimulants representing humoral immunity and allergy disorders (Dong, 2008). This was demonstrated by Ocmant et al. who measured an allergen-specific IL-4 response with real-time PCR from cat allergic patients. (Ocmant et al., 2005)

6.4. Limitations of the study

The limitations of this study concern the restricted amount of the white blood cell samples obtained from the DIPP study, the limited number of cytokines studied and the absence of cytokine protein analyses. The samples of the DIPP biobank are unique. Therefore, the consumption of the buffy-coat samples to RNA isolation experiments was limited to avoid the wasting of the samples. The real-time PCR panel developed in this study covers only a part of all the cytokines and so it gives a limited picture about the immune system. On the other hand, the most important cytokines describing the three proinflammatory cell lineages were included. The mRNA expression may not be linearly related to the translation of these cytokines. Thus, it would also be important to detect and analyze the proteins to obtain a relevant general view. However, unlike similar real-time PCR methods, this panel is not sensitive to genomic-DNA contamination.

6.5. Future aspects

The real-time PCR methods which were developed for the detection of proinflammatory cytokines, IFN-γ, IL-4 and IL-17, can be used to analyze the cytokine expression from human white blood cells in the DIPP study. This method fulfils the requirements which were set at the beginning of the project being sensitive, specific and applicable for both mononuclear cell and buffy-coat samples. The successful RNA isolation from buffy-coat samples enables the efficient utilization of the DIPP biobank in future studies evaluating immunopathogenesis of type 1 diabetes and related immune-mediated diseases. The methods are also suitable for the analysis of *in vitro* responses of white blood cells to viruses and other antigens which can play a role in the pathogenesis of type 1 diabetes. Such studies may indentify immunological pathways leading to the imbalance of the immune system towards T_H1, T_H2 or T_H17 pathways in these diseases.

7. CONCLUSIONS

This study aimed at developing real-time PCR method to study the function of proinflammatory T cells in immune-mediated diseases. An additional aim was to develop an RNA isolation method, which would work for frozen buffy-coat samples collected in large-scale epidemiological studies and stored for years in freezers. Immune-mediated diseases, such as type 1 diabetes, are associated with an unbalanced function of proinflammatory T cells. Moreover, virus infections, which can cause abnormalities in the function of these T cells, have been connected to the pathogenesis of immune-mediated diseases. This study created RNA isolation and real-time PCR methods which can be directly applied in this kind of studies to analyze the role of cytokine expression and role of virus infections in the pathogenesis of type 1 diabetes.

REFERENCES

Akdis M. Healthy immune response to allergens: T regulatory cells and more. Current Opinion in Immunology 2006;18:738-744.

Alberts B, Johnson A, Lewis J, Raff M, Roberts K, Walter P. Molecular biology of the cell, Garland Science, New York, 2002, pp. 317-319 and 494-495.

Bach JF. The effect of infections on susceptibility to autoimmune and allergic diseases. N Eng J Med 2002;347:911-920.

Beyan H, Buckley LR, Yousaf N, Londel M, Leslie RDG. A role of innate immunity in type 1 diabetes? Diabetes/Metabolism Research and Reviews 2003;19:89-100.

Bullens D, Truyen E, Coteur L, Dilissen E, Hellings PW, Dupont LJ, Ceupens JL. IL-17 mRNA in sputum of asthmatic patients: linking T cell driven inflammation and granulocytic influx? Respirtory research 2006;7:1-9.

Bustin SA. Absolute quantification of mRNA using real-time reverse transcription polymerase chain reaction assays. Journal of Molecular Endocrinology 2000;25:169-193.

Chatila TA, Li N, Garcia-Lloret M, Kim HJ, Nel AE. T-cell effector pathways in allergic diseases: transcriptional mechanisms and therapeutic targets. Journal of Allergy Clinical Immunoloygy 2008;121:812-823.

Coëffier M, Lorenyz A, Manns MP, Bischoff SC. Epsilon germ-line and IL-4 transcripts are expressed in human intestinal mucosa and enhanced in patients with food allergy. Allergy 2005;60:822-827.

Cools N, Ponsaert P, Van Tendeloo V, Berneman ZN. Regulatory T cells and human disease. Clinical and Developmental Immunology 2007;2007:1-11. Published online (Article ID 89195).

Dong C. T_H17 cells in development: an updated view of their molecular identity and genetic programming. Nature Reviews Immunology 2008;8:337-348.

Gamble DR, Kinsley ML, FitzGerald MG, Bolton R, Taylor KW. Viral antibodies in diabetes mellitus. Br Med J 1969;3:627-630.

Isomäki P, Alanärä T, Isohanni P, Lagerstedt A, Korpela M, Moilanen T, Visakorpi T, Silvennoinen O. The expression of SOCS is altered in rheumatoid arthritis. Rheumatology (Oxford) 2007;46;1538-1546.

Janeway CA, Travers P, Walport M, Shlomchik MJ. Immunobiology – the immune system in health and diseases. Garland Science, New York, 2005, pp. 341, 517-518 and 557-560.

Knip M, Veijola R, Virtanen SM, Hyöty H, Vaarala O, Åkerblom HK. Environmental triggers and determinants of type 1 diabetes. Diabetes 2005;54:125-136.

Kondrashova A, Mustalahti K, Kaukinen K, Viskari H, Volodicheva V, Haapala AM, Ilonen J, Knip M, Mäki M, Hyöty H and the EPIVIR Study Group. Lower economic status and inferior hygienic environment may protect against celiac disease. Ann Med 2008a;40:223-231.

Kondrashova A, Romanov A, Reunanen A, Karvonen A, Viskari H, Vesikari T, Ilonen J, Knip M, Hyöty H. A six-fold gradient in the incidence of type 1 diabetes at the eastern border of Finland – evidence of a critical role of environment in the disease pathogenesis. Annals of Medicine 2005;37: 67-72.

Kondrashova A, Viskari H, Haapala AM, Seiskari T, Kulmala P, Ilonen J, Knip M, Hyöty H. Serological evidence of thyroid autoimmunity among schoolchildren in two different socioeconomic environments. J Clin Endocrinol Metab. 2008b;93:729-73.

Kondrashova A, Viskari H, Kulmala P, Romanov A, Ilonen J, Hyöty H, Knip M. Signs of beta-cell autoimmunity in non–diabetic schoolchildren: A comparison between Russian Karelia with a low incidence of Type 1 diabetes and Finland with a high incidence rate. Diabetes Care 2007;30:95-100.

Kubista M, Andrade JM, Bengtsson M, Forootan A, Jonal J, Lind K, Sindelka R, Sjöback R, Sjögreen B, Strömbom L, Ståhlberg A, Zoric N. The real-time polymerase chain reaction. Molecular Aspects of Medicine 2006;27:95-125.

Kupila A, Muona P, Simell T, Arvilommi P, Savolainen H, Hämäläinen AM, Korhonen S, Kimpimäki T, Sjöroos M, Ilonen J, Knip M, Simell O. Feasibility of genetic and immunological prediction of type 1 diabetes in a population-based birth cohort. Diabetologia 2001;44:290-297.

Kurts C. Th17 cells: a third subset of CD4+ T effector cells involved in organ-specific autoimmunity. Nephrol Dial Transplant 2008;23:816-819.

Kvandström M, Jenmalm M, Ekerfelt C. Effect of cryopreservation on expression of Th1 and Th2 cytokines in blood mononuclear cells from patients with different cytokine profiles, analysed with three common assays: an overall decrease of interleukin-4. Cryobiology 2004;49:157-168.

Li L, Dufour A. Using IFN-γ as a biomarker for detecting exposure to viral pathogens. Curr Microbiol 2008;56:84-88.

Mackay IM, Arden KE, Nitsche A. Real-time PCR in virology. Nucleic Acids Research 2002;30:1292-1305.

Nakae S, Komiyama Y, Nambu A, Sudo K, Iwase M, Homma I, Sekikawa K, Asano M, Iwakura Y. Antigen-specific T cell sensitization is impaired in IL-17-deficient mice, causing suppression of allergic cellular and humoral responses. Immunity 2002;17:375-387.

Nakae S, Nambu A, Sudo K, Iwakura Y. Suppression of immune induction of collagen-induced arthritis in IL-17-deficient mice. J Immunol 2003;171:6173-6177.

Näntö-Salonen S, Kupila A, Simell S, Siöjader H, Salonkaari T, Hekkala A, Korhonen S, Erkkola R, Sipilä J, Haavisto L, Siltala M, Tuominen J, Hakalax J, Hyöty H, Ilonen J, Veijola R, Simell T, Knip M, Simell O. Nasal insulin to prevent type 1 diabetes in children with HLA genotypes and

autoantibodies conferring increased risk of disease: a double-blind, randomised controlled trial. Lancet. 2008;15:1746-1755.
Oboki K, Ohno T, Saito H, Nakae S. Th17 and allergy. Allergology International 2008;57:121-134.

Ocmant A, Michils A, Schandene´ L, Peignois Y, Goldman M, Patrick Stordeur P. IL-4 and IL-13 mRNA real-time PCR quantification on whole blood to assess allergic response. Cytokine 2005;31:375-381.

Oikarinen M, Tauriainen S, Honkanen T, Oikarinen S, Vuori K, Kaikinen K, Rantala I, Mäki M, Hyoty H. Detection of enteroviruses in the intestine of type 1 diabetic patients. Clinical and Experimental Immunology 2007;151:71-75.

Pfaffl M. A new mathematical model for relative quantification in real-time RT-PCR. Nucleic Acids Research 2001;29:2002-2007.

Rabin RL, Levinson AI. The nexus between atopic disease and autoimmunity: a review of the epidemiological and mechanistic literature. Clinical and Experimental Immunology 2008;153:19-30.

Rautajoki KJ, Kyläniemi MK, Raghav SK, Rao K, Lahesmaa R. An insight into molecular mechanisms of human T helper cell differentiation. Annals of Medicine 2008;40:322-335.

Richman DD, Whitney RJ, Hayden FG. Clinical virology, ASM Press, Washington, 2002, pp. 971-983 and 984.

Rouse BT. Regulatory T cells in health and disease. Journal of Internal Medicine 2007;262:78-95.

Seiskari T, Kondrashova A, Viskari H, Kaila M, Haapala AM, Aittoniemi J, Virta M, Hurme M, Uibo R, Knip M, Hyöty H, EPIVIR study group. Allergic sensitization and microbial load – a comparison between Finland and Russian Karelia. Clinical and Experimental Immunology 2007;148:47-52.

Tauriainen S, Salminen K, Hyöty H. Can enteroviruses cause type 1 diabetes? Annals New York Academy of Sciences 2003;1005:13-22.

Valasek MA, Repa JJ. The power of real-time PCR. The American Physiological Society 2005;29:151-159.

van der Werf N, Kroese F, Rozing J, Hillebrans JL. Viral infections as potential triggers of type 1 diabetes. Diabetes/Metabolism Research and Reviews 2007;23:169-183.

Viskari H, Ludvigsson J, Uibo R, Salur L, Marciulionyte D, Hermann R, Soltesz G, Fuchtenbuch M, Ziegler AG, Kondrashova A, Romanov A, Knip M, Hyöty H. Relationships between the incidence of type 1 diabetes and enterovirus infections in different European populations: results from the EPIVIR project. Journal of Medical Virology 2004;7:610-617.

Wang DY. Risk factors of allergic rhinitis: genetic or environmental? Therapeutics and Clinical Risk Management 2005;1:115-123.